ELSEVIER

Journal of Organometallic Chemistry 578 (1999) 3–30

Journal of Organometallic Chemistry

Review

Luminescent polynuclear metal acetylides

Vivian Wing-Wah Yam *, Kenneth Kam-Wing Lo, Keith Man-Chung Wong

Department of Chemistry, The University of Hong Kong, Pokfulam Road, Hong Kong, PR China

Received 2 July 1998

Abstract

The photophysical and photochemical studies of polynuclear copper(I), silver(I), gold(I), rhenium(I) and platinum(II) acetylide complexes are reviewed. Based on the highly flexible bonding modes of the acetylides and the various coordination geometry of these metal centres, a number of polynuclear copper(I), silver(I), gold(I), rhenium(I) and platinum(II) acetylide complexes with very different molecular structures have been synthesized and characterized. These organometallic complexes also exhibit rich and remarkable photophysical and photochemical properties which are unique to the presence of the acetylide ligand. The fundamental understanding on the photophysical and photochemical properties of these luminescent organometallic complexes would lead to the production of novel luminescent materials and represent model systems in the development of light-emitting diodes, new materials with non-linear optical properties and liquid crystalline properties. In this review article, particular attention is focused on the electronic absorption spectroscopy, photoluminescence behaviour, excited-state assignments and photochemical properties of this class of luminescent acetylide complexes.

Keywords: Acetylides; Copper(I); Gold(I); Luminescence; Photoredox; Platinum(II); Rhenium(I); Silver(I)

1. Introduction

The present article focuses on our recent efforts in the design and synthesis of luminescent polynuclear metal acetylides of selected metal centres and the photophysical aspects of these classes of compounds. The chemistry of metal acetylides has attracted enormous attention, in particular, with the emerging interest in their potential applications in the field of materials science. The linear geometry of the acetylide unit and its π-unsaturated nature have made the metal acetylides attractive building blocks for molecular wires and organometallic oligomeric and polymeric materials which may possess unique properties such as optical nonlinearity, electrical conductivity, and liquid crystallinity. Despite the growing interests and extensive studies in metal acetylides, relatively less attention was focused on the luminescence behaviour of this class of compounds. In this context, we have directed our research specifically to the design and synthesis of luminescent metal acetylides and, with a judicious choice, of employing them as versatile building blocks for luminescent oligomeric materials.

Abbreviations: Bpy, 2,2′-bipyridine; $^{t}Bu_2$bpy, 4,4′-di-*t*-butyl-2,2′-bipyridine; Dcpn, 1,8-bis(dicyclohexylphosphino)naphthalene; Dmb, 1,8-diisocyano-*p*-menthane; Dmmp, bis(dimethylphosphinomethyl)-methylphosphine; Dmpe, bis(dimethylphosphino)ethane; Dmpm, bis(dimethylphosphino)methane; Dpmp, 2-(diphenylmethyl)pyridine; Dppe, 1,2-bis(diphenylphosphino)ethane; Dppf, 1,1′-bis(diphenylphosphino)ferrocene; Dppm, bis(diphenylphosphino)methane; Dppn, 1,8-bis(diphenylphosphino)naphthalene; Dpppy, 2,6-bis(diphenylphosphino)pyridine; Dppy, 2-diphenylphosphinopyridine; Dptact, 1,4,8,11-tetra(diphenylphosphinomethyl)-1,4,8,11-tetraazacyclotetradecane; Fc, ferrocene; IL, intraligand; LC, ligand-centred; LMCT, ligand-to-metal charge-transfer; MC, metal-centred; MLCT, metal-to-ligand charge-transfer; MMLCT, metal–metal-bond-to-ligand charge-transfer; MV^{2+}, methyl viologen; Np, 1-naphthyl; SSCE, saturated sodium chloride calomel electrode; Tmb, 2,5-diisocyano-2,5-dimethylhexane.

* Corresponding author.

0022-328X/99/$ - see front matter
PII: S0022-328X(98)01106-1

2. Copper(I), silver(I) and gold(I) acetylides

2.1. Copper(I) acetylides

The chemistry of the organocopper species is of great importance owing to their wide applications in organic chemistry [1–4]. In addition to the aryl and alkyl derivatives, copper(I) acetylides have also been arousing a lot of interest due to the highly flexible bonding modes of the acetylides [5,6]. One of the most common bonding modes of the acetylide is the μ_3-η^1 type. The synthesis and crystal structures of *triangulo* copper(I) acetylides $[Cu_3(\mu\text{-dppm})_3(\mu_3\text{-}\eta^1\text{-}C{\equiv}C{-}Ph)]^{2+}$ [7] and $[Cu_3(\mu\text{-dppm})_3(\mu_3\text{-}\eta^1\text{-}C{\equiv}C{-}Ph)_2]^{+}$ [8] were first reported by Gimeno and coworkers. The interesting photophysical and photochemical properties of a number of luminescent polynuclear copper(I) acetylide complexes have recently been reported by us [9–21]. The first series of these compounds is the trinuclear system with one or two μ_3-η^1-bridging acetylide ligands $[Cu_3(\mu\text{-dppm})_3(\mu_3\text{-}\eta^1\text{-}C{\equiv}C{-}R)_2]^{+}$ [R = Ph (**1a**), ^{t}Bu (**1b**), $C_6H_4{-}NO_2$-4 (**1c**), $C_6H_4{-}$Ph-4 (**1d**), $C_6H_4{-}OCH_3$-4 (**1e**), $C_6H_4{-}NH_2$-4 (**1f**), $^nC_6H_{13}$ (**1g**)] and $[Cu_3(\mu\text{-dppm})_3(\mu_3\text{-}\eta^1\text{-}C{\equiv}C{-}R)]^{2+}$ [R = Ph (**2a**), ^{t}Bu (**2b**), $C_6H_4{-}NO_2$-4 (**2c**), $C_6H_4{-}$Ph-4 (**2d**), $C_6H_4{-}OCH_3$-4 (**2e**), $C_6H_4{-}NH_2$-4 (**2f**), $^nC_6H_{13}$ (**2g**)] [11–13,21]. Besides, the luminescence properties of mixed-capped trinuclear copper(I) acetylide complexes $[Cu_3(\mu\text{-dppm})_3(\mu_3\text{-}\eta^1\text{-}C{\equiv}C{-}^t\text{Bu})(\mu_3\text{-Cl})]^{+}$ (**3a**) [11], $[Cu_3(\mu\text{-dppm})_3(\mu_3\text{-}\eta^1\text{-}C{\equiv}C{-}C_6H_4{-}OCH_3\text{-}4)(\mu_3\text{-}\eta^1\text{-}C{\equiv}C{-}C_6H_4{-}OCH_2CH_3\text{-}4)]^{+}$ (**3b**) [20] and $[Cu_3(\mu\text{-dppm})_3(\mu_3\text{-}\eta^1\text{-}C{\equiv}C{-}C_6H_4{-}OCH_3\text{-}4)(\mu_2\text{-}\eta^1\text{-}C{\equiv}C{-}C_6H_4{-}NO_2\text{-}4)]^{+}$ (**3c**) [20] have also been studied. Some of these complexes have been structurally characterized. The perspective view of the complex cation of **1e** is depicted in Fig. 1. The Cu···Cu distances of these copper(I) acetylides and related complexes are collected in Table 1.

The electronic absorption bands at ca. 252–268 and 292–328 nm of these trinuclear copper(I) acetylides have been assigned to ligand-centred π–π^*(dppm) and π–π^*(acetylide) transitions, respectively, owing to the similar absorption energies with those of the free dppm ligand and acetylenes. In addition, there are also lower energy absorption bands at ca. 332–404 nm. The energy of this absorption band has been found to be in line with the π–π^* transition energy of the acetylide. For example, the 4-nitrophenylacetylide mono-capped complex **2c** (396 nm) absorbs at lower energy than the 1-octynyl counterpart **2g** (332 nm) [21]. This observation suggests that this low energy absorption band is a metal-perturbed ligand-centred π–π^*(acetylide) or a MLCT [d(Cu) $\rightarrow$ π^*(acetylide)] transition, or an admixture of both.

Excitation of these complexes in the solid state and in fluid solutions results in long-lived and intense luminescence. The photophysical data are listed in Table 2. Some of the complexes show vibronically structured emission bands with vibrational progressional spacings of ca. 1350–1600 and ca. 1800–2000 cm^{-1}, which are typical of ground-state aromatic ν(C=C) and acetylide ν(C≡C) stretching frequencies. This observation is suggestive of the involvement of acetylides in the excited states of these complexes. The lifetimes are in the microsecond range, suggesting that the luminescence is associated with a spin-forbidden transition. In general, the complexes with electron-rich acetylides emit at a lower energy. For example, the emission energies of $[Cu_3(\mu\text{-dppm})_3(\mu_3\text{-}\eta^1\text{-}C{\equiv}C{-}R)]^{2+}$ in acetone solution follow the order: R = $C_6H_4{-}OCH_3$-4 (483 nm) $\simeq$ Ph (499 nm) $\simeq$ $C_6H_4{-}NH_2$-4 (504, 564 nm) > ^{t}Bu (640 nm) $\simeq$ $^nC_6H_{13}$ (650 nm) [13,21]. This is in line with the increasing donating ability of the acetylide ligand. Therefore, the origin of the emission has been proposed to involve substantial ligand-to-metal charge-transfer LMCT [acetylide $\rightarrow$ Cu_3] character. However, in view of the short Cu···Cu distances found in the trinuclear copper(I) complexes, especially in the case of the bi-capped acetylide species, it is likely that the lowest-lying emissive state is mixed with some metal-centred $3d^94s^1$ character. Besides, the mono-capped species have been found to emit at a lower energy than the bi-capped analogues with the same acetylide ligand [11,13,21]. It is

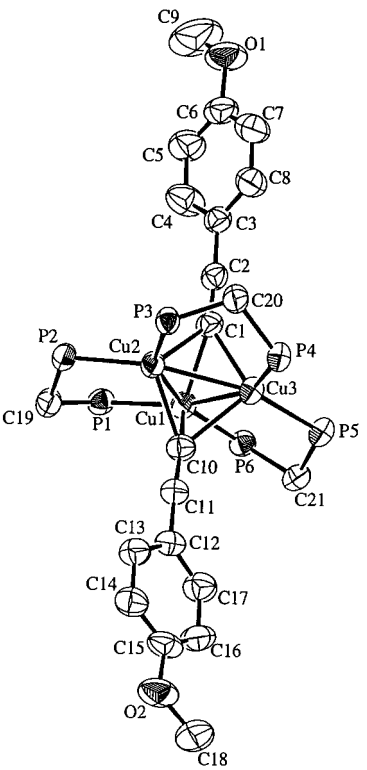

Fig. 1. The perspective view of the complex cation of **1e**. Hydrogen atoms and phenyl rings have been omitted for clarity.

Table 1
Cu···Cu distances of selected polynuclear copper(I) acetylide complexes

Complex	Cu···Cu (Å)	Reference
$[Cu_3(\mu\text{-dppm})_3(\mu_3\text{-}\eta^1\text{-}C{\equiv}C\text{–}Ph)_2]^+$ (**1a**)	2.570(3)–2.615(3)	[8]
$[Cu_3(\mu\text{-dppm})_3(\mu_3\text{-}\eta^1\text{-}C{\equiv}C\text{–}C_6H_4\text{–}OCH_3\text{-}4)_2]^+$ (**1e**)	2.5862(9)–2.6174(8)	[21]
$[Cu_3(\mu\text{-dppm})_3(\mu_3\text{-}\eta^1\text{-}C{\equiv}C\text{–}Ph)]^{2+}$ (**2a**)	2.813(3)–3.274(3)	[7]
$[Cu_3(\mu\text{-dppm})_3(\mu_3\text{-}\eta^1\text{-}C{\equiv}C\text{–}^t\!Bu)]^{2+}$ (**2b**)	2.910(1)–3.175(1)	[13]
$[Cu_3(\mu\text{-dppm})_3(\mu_3\text{-}\eta^1\text{-}C{\equiv}C\text{–}^t\!Bu)(\mu_3\text{-}Cl)]^+$ (**3a**)	2.754(2)–2.927(2)	[11]
$[Cu_3(\mu\text{-dppm})_3(\mu_3\text{-}\eta^1\text{-}C{\equiv}C\text{–}C_6H_4\text{–}OCH_3\text{-}4)(\mu_3\text{-}\eta^1\text{-}C{\equiv}C\text{–}C_6H_4\text{–}OCH_2CH_3\text{-}4)]^+$ (**3b**)	2.574(1)–2.621(1)	[20]
$[Cu_3(\mu\text{-dppm})_3(\mu_3\text{-}\eta^1\text{-}C{\equiv}C\text{–}C_6H_4\text{–}OCH_3\text{-}4)(\mu_2\text{-}\eta^1\text{-}C{\equiv}C\text{–}C_6H_4\text{–}NO_2\text{-}4)]^+$ (**3c**)	2.557(1)–2.758(1)	[20]
$[Cu_4(PPh_3)_4(\mu_3\text{-}\eta^1\text{-}C{\equiv}C\text{–}C_6H_4\text{–}OCH_3\text{-}4)_4]$ (**5b**)	2.5241(8)–2.6636(8)	[21]
$[Cu_4(PPh_3)_4(\mu_3\text{-}\eta^1\text{-}C{\equiv}C\text{–}Ph)_4]$ (**5e**)	2.523(1)–2.676(1)	[34]
$[Cu_4\{P(C_6H_4\text{-}F\text{-}4)_3\}_4(\mu_3\text{-}\eta^1\text{-}C{\equiv}C\text{–}Ph)_4]$ (**5f**)	2.550(2)–2.648(2)	[14]
$[Cu_4\{P(C_6H_4\text{–}CH_3\text{-}4)_3\}_4(\mu_3\text{-}\eta^1\text{-}C{\equiv}C\text{–}Ph)_4]$ (**5g**)	2.567(2)–2.607(2)	[14]
$[Cu_4(PPh_3)_4(\mu_3\text{-}\eta^1,\eta^1,\eta^2\text{-}C{\equiv}C\text{–}C_6H_4\text{–}OCH_3\text{-}4)_3]^+$ (**6**)	2.446(2)–2.467(2)	[15]
$[Cu_4(\mu\text{-dppm})_4(\mu_4\text{-}\eta^1,\eta^2\text{-}C{\equiv}C)]^{2+}$ (**7**)	3.245(2), 3.264(2)	[16]
$[Cu_2(PPh_2CH_3)_2(\mu,\eta^1\text{-}C{\equiv}C\text{–}Ph)_2]$ (**8**)	2.454(1)	[17]
$[Cu_3(\mu\text{-dppm})_3(\mu_3\text{-}\eta^1\text{-}C{\equiv}C\text{–}C_6H_4\text{–}C{\equiv}C\text{-}4)Cu_3(\mu\text{-dppm})_3]^{4+}$ (**9**)	2.862(2)–3.243(1)	[19]
$[Cu_3(\mu\text{-dppm})_3\{\mu_3\text{-}\eta^1\text{-}C{\equiv}C\text{–}C_6H_4\text{–}C{\equiv}C\text{-}4\text{–}Re(bpy)(CO)_3\}_2]^+$ (**36a**)	2.556(2)–2.674(3)	[138]

likely that the higher overall positive charge of the mono-capped acetylide complexes relative to those of the bi-capped species would stabilize the essentially metal-centred LUMO, leading to a lower-lying LMCT emissive state. Overall speaking, the lowest-lying emissive state could be best described as an admixture of the LMCT triplet state and a metal-centred $3d^94s^1$ state modified by copper–copper interactions. The relative degrees of the LMCT and MC character depend on the nature of the acetylide ligand as well as the extent of metal–metal interaction. However, for the complexes containing acetylide ligands with electron-withdrawing substituents, such as 4-nitrophenylacetylide [20,21], the emission bands are very similar to that of the uncoordinated acetylene units. It is likely that some ligand-centred π–π^*(acetylide) character is also involved in the emissive state of these complexes.

In order to examine the effects of the bridging phosphine ligands, a series of related bi-capped trinuclear copper(I) acetylides with PNP [bis(diphenylphosphino)-alkyl and -aryl amine] ligands have also been synthesized and their photophysical and photochemical properties studied [18]. These complexes can be represented by the general formula $[Cu_3\{\mu\text{-}(Ph_2P)_2N\text{–}R\}_3(\mu_3\text{-}\eta^1\text{-}C{\equiv}C\text{–}R')_2]^+$ [$R = CH_2CH_2CH_3$, $R' = C_6H_4\text{–}OCH_2CH_3$-4 (**4a**), $R' = C_6H_4\text{–}$Ph-4 (**4b**), $R' =$ Ph (**4c**), $R' = C_6H_4\text{–}NO_2$-4 (**4d**); $R =$ Ph, $R' = C_6H_4\text{–}OCH_2CH_3$-4 (**4e**), $R' = C_6H_4\text{–}$Ph-4 (**4f**), $R' =$ Ph, (**4g**), $R' = {}^nC_6H_{13}$ (**4h**); $R = C_6H_4\text{–}CH_3$-4, $R' = C_6H_4\text{–}OCH_2CH_3$-4 (**4i**); $R = C_6H_4\text{–}$F-4, $R' = C_6H_4\text{–}$Ph-4 (**4j**)]. The complexes also display long-lived and intense luminescence upon photoexcitation. The photophysical data are collected in Table 3. It has been suggested that the low energy emission originates from a LMCT [acetylide $\rightarrow Cu_3$] excited state mixed with a copper-centred d-s state based on the observed trend in the emission energies of the complexes in the order **4g** > **4e** > **4h**, which is in line with the increasing electron-donating abilities of the acetylides. The role played by the bridging phosphine ligands has also been studied. It has been found that the low energy emission for the 4-ethoxyphenylacetylide complexes with different phosphine ligands follows the order: **4a** > **4i** > **4e**. This observation is in agreement with the assignment of an excited state with substantial LMCT [acetylide $\rightarrow Cu_3$] or LLCT [acetylide $\rightarrow \pi^*$(phosphine)] character in which the electron richness of the PNP ligands follows the order: $R = CH_2CH_2CH_3 > C_6H_4\text{–}CH_3$-4 > Ph. However, an excited state of LLCT parentage is not likely in view of the small changes in the energies along the series. On the other hand, the emission spectra of the biphenylacetylide complexes (**4b**, **4f** and **4j**) reveal very similar vibronically structured bands. The observed vibrational progressional spacings of ca. 1400–1500 cm^{-1} are typical of the $\nu(C{\cdots}C)$ stretching frequencies of the aromatic rings. Besides, the emission band of **4d** in low-temperature glass occurs at 671 nm, which is similar to that observed for uncoordinated 4-nitrophenylacetylene. For these complexes with the relatively electron-deficient biphenyl- and 4-nitrophenyl-acetylide ligands, it is likely that substantial intraligand $^3[\pi \rightarrow \pi^*$(acetylide)] character is involved in the excited state.

These trinuclear copper(I) acetylide complexes have been found to exhibit rich photoredox properties. For example, the emission of **2b** is quenched in the presence of a series of structurally related pyridinium ions [13]. The triplet-state energies of the pyridinium ions are too high for any energy transfer reactions to occur. From the dependence of the bimolecular quenching rate constants on the reduction potentials of the pyridinium quenchers, it has been suggested that the quenching is associated with an oxidative electron-transfer mecha-

nism. The photoinduced electron transfer reaction has also been confirmed by nanosecond transient absorption spectroscopy [12,13,18,21]. For example, the transient absorption difference spectrum recorded 10 μs after laser flash excitation of **1a** (0.05 mM) and 4-(methoxycarbonyl)-*N*-methylpyridinium hexafluorophosphate (13 mM) in degassed acetonitrile (0.1 M $^{n}Bu_4NPF_6$) is displayed in Fig. 2. The sharp absorption band at 400 nm is characteristic of the pyridinyl radical [22,23]. This observation indicates that the photoreaction involves the reduction of the pyridinium cation to the pyridinyl radical, meanwhile **1a*** is oxidised to a mixed-valence transient species $[Cu(I)Cu(I)Cu(II)]^{2+}$. The reaction mechanism is likely to be:

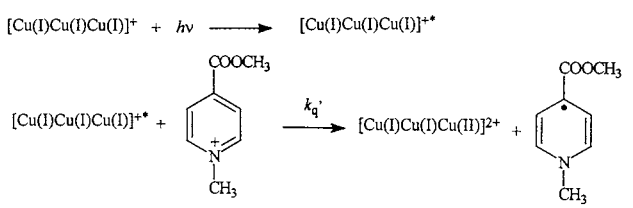

Table 2
Photophysical data for **1a**–**g**, **2a**–**g**, and **3a**–**c**

Complex	Medium (T/K)	Emission wavelength λ_{max}/nm (τ_o/μs)	Reference
1a	Solid (298)	493 (14 ± 1)	[13]
	Solid (77)	485, 525 sh	
	Acetone (298)	495 (5.9 ± 0.5)	
1b	Solid (298)	450 (0.44 ± 0.05), 540 (1.7 ± 0.2)	[13]
	Solid (77)	450, 530 sh	
	Acetone (298)	444 (0.24 ± 0.02), 580 sh (16 ± 1)	
1c	Solid (298)	420 (0.21)	[21]
	Solid (77)	630	
	Acetone (298)	438, 469 (1.5)	
1d	Solid (298)	527, 562 sh (5.7)	[21]
	Solid (77)	532, 574	
	Acetone (298)	530, 570 sh (16.3)	
1e	Solid (298)	450, 482 (63.8)	[21]
	Solid (77)	450, 478, 490 sh, 525	
	Acetone (298)	481 (11.5)	
1f	Solid (298)	402 (0.3)	[21]
	Solid (77)	485, 521 sh, 567 sh	
	CH_2Cl_2 (298)	476, 515 sh (4.0)	
1g	Solid (298)	444 (3.6)	[21]
	Solid (77)	455	
	Acetone (298)	455, 600 sh (1.0)	
2a	Solid (298)	500 (21 ± 2)	[13]
	Solid (77)	492, 530 sh	
	Acetone (298)	499 (6.8 ± 0.7)	
2b	Solid (298)	627 (14 ± 1)	[13]
	Solid (77)	450, 570 sh, 692	
	Acetone (298)	640 (2.6 ± 0.3)	
2c	Solid (298)	590 (128.0)	[21]
	Solid (77)	587, 640 sh	
	Acetone (298)	464, 654 (2.1)	
2d	Solid (298)	529, 572 sh (360.0)	[21]
	Solid (77)	530, 573 sh	
	Acetone (298)	533 (23.9)	
2e	Solid (298)	471, 523 sh, 585 (2.9)	[21]
	Solid (77)	495, 538 sh, 600 sh	
	Acetone (298)	483 (5.5)	
2f	Solid (298)	418 (3.5)	[21]
	Solid (77)	508	
	Acetone (298)	504, 564 sh (4.8)	
2g	Solid (298)	601 (24.4)	[21]
	Solid (77)	540 sh, 640	
	Acetone (298)	650 (1.54)	
3a	Solid (298)	440 sh (<0.01), 535 (33 ± 3)	[11]
	Solid (77)	440, 572	
	CH_3CN (298)	540 sh (5.3 ± 0.5), 613 (5.4 ± 0.5)	
3b	Solid (298)	475, 502 (17.6)	[20]
	Solid (77)	467, 515, 569	
	Acetone (298)	479 (5.6)	
3c	Solid (298)	671 (0.2)	[20]
	Solid (77)	697	
	Acetone (298)	489 (3.6)	

Table 3
Photophysical data for **4a**–**j**[a]

Complex	Medium (T/K)	Emission wavelength λ_{max}/nm (τ_o/μs)
4a	Solid (298)	459 (3.1)
	Solid (77)	453 sh, 482
	Acetone (298)	467 (4.4)
4b	Solid (298)	521, 558 sh, 615 sh (6.6)
	Solid (77)	522, 565, 615 sh
	Acetone (298)	516, 554, 615 sh (26.1)
4c	Solid (298)	461 (4.0)
	Solid (77)	459, 485, 495, 507
	Acetone (298)	465 (3.4)
4d	Solid (298)	400 (4.0)
	Solid (77)	400
	Acetone (298)	454 (1.6)
4e	Solid (298)	469 (0.3)
	Solid (77)	493
	Acetone (298)	484, 646 (7.0)
4f	Solid (298)	467, 516, 550 sh (5.5)
	Solid (77)	515, 560, 615 sh
	Acetone (298)	516, 552, 615 sh (35.0)
4g	Solid (298)	464, 550 sh (5.6)
	Solid (77)	462 sh, 487
	Acetone (298)	461, 633 (4.8)
4h	Solid (298)	418, 438 sh, 467 (1.2)
	Solid (77)	501
	Acetone (298)	471, 670 (3.4)
4i	Solid (298)	466, 550 sh (4.8)
	Solid (77)	491
	Acetone (298)	464, 632 (2.5)
4j	Solid (298)	471, 516, 545, 615 sh (6.3)
	Solid (77)	516, 556, 615 sh
	Acetone (298)	470 sh, 568 (30.0)

[a] Data from reference [18].

Apart from the 400-nm absorption, a broad absorption band at ca. 810 nm ($\varepsilon = 9940$ dm^3 mol^{-1} cm^{-1}) has also been observed in the transient absorption difference spectrum [12]. As the pyridinyl radical does not absorb in this region, this low energy absorption has been suggested to arise from the one-electron oxidised species **1a**$^+$. The possibility of ligand-field transitions of Cu(II) is not favoured owing to the high extinction coefficient of this absorption band [24]. Instead, this broad absorption band has been assigned to arise from an intervalence-transfer IT transition:

$$\mathrm{Cu(I)Cu(I)Cu(II)} \xrightarrow{h\nu} \mathrm{Cu(I)Cu(II)Cu(I)^*}$$

Similar intervalence-transfer transitions have also been reported for a number of mixed-valence copper(I,II) systems [25–31].

A plot of $1/\Delta A$ versus time gave a straight line (Fig. 2 inset), indicating that the decay follows second-order kinetics, corresponding to the back electron-transfer reaction:

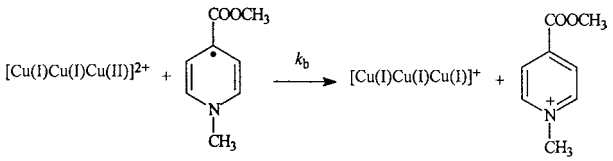

A back electron-transfer rate constant k_b for this reaction has been estimated to be 2.3×10^{10} dm^3 mol^{-1} s^{-1}.

Similar low energy intervalence-transfer transitions have also been observed for other trinuclear copper(I) acetylides **1b** [12], **1e** [21], **2b** [13], **3a** [12], **4c** [18] and a series of tetranuclear copper(I) chalcogenides $[Cu_4(\mu\text{-}Ar_2PCH_2PAr_2)_4(\mu_4\text{-}E)]^{2+}$ (Ar = Ph, E = S, Se; Ar = C_6H_4–CH_3-4, E = S) with different pyridinium acceptors [32,33].

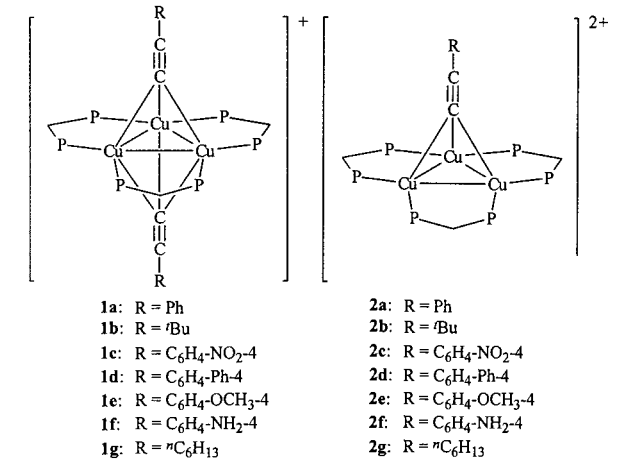

1a: R = Ph
1b: R = ^{t}Bu
1c: R = C_6H_4-NO_2-4
1d: R = C_6H_4-Ph-4
1e: R = C_6H_4-OCH_3-4
1f: R = C_6H_4-NH_2-4
1g: R = $^n C_6H_{13}$

2a: R = Ph
2b: R = ^{t}Bu
2c: R = C_6H_4-NO_2-4
2d: R = C_6H_4-Ph-4
2e: R = C_6H_4-OCH_3-4
2f: R = C_6H_4-NH_2-4
2g: R = $^n C_6H_{13}$

P P = dppm

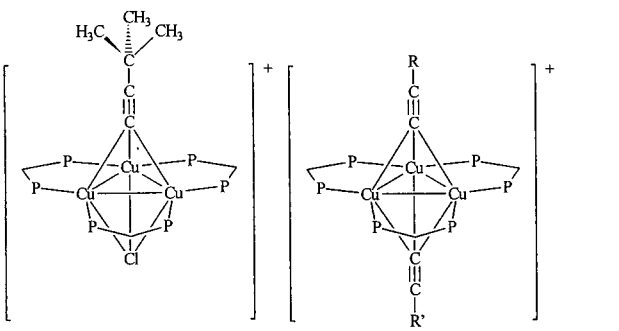

3a

3b: R = C_6H_4-OCH_3-4, R' = C_6H_4-OCH_2CH_3-4
3c: R = C_6H_4-OCH_3-4, R' = C_6H_4-NO_2-4

P P = dppm

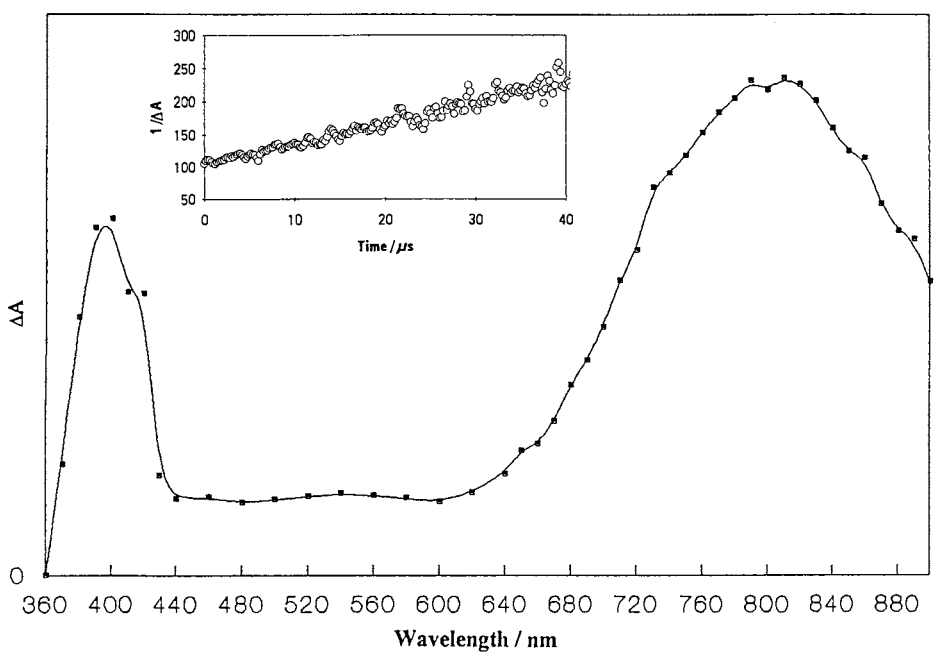

Fig. 2. The transient absorption difference spectrum recorded 10 μs after laser flash excitation of **1a** (0.05 mM) and 4-(methoxycarbonyl)-*N*-methylpyridinium hexafluorophosphate (13 mM) in degassed acetonitrile (0.1 M $^n Bu_4NPF_6$). Inset: a plot of $1/\Delta A$ versus time.

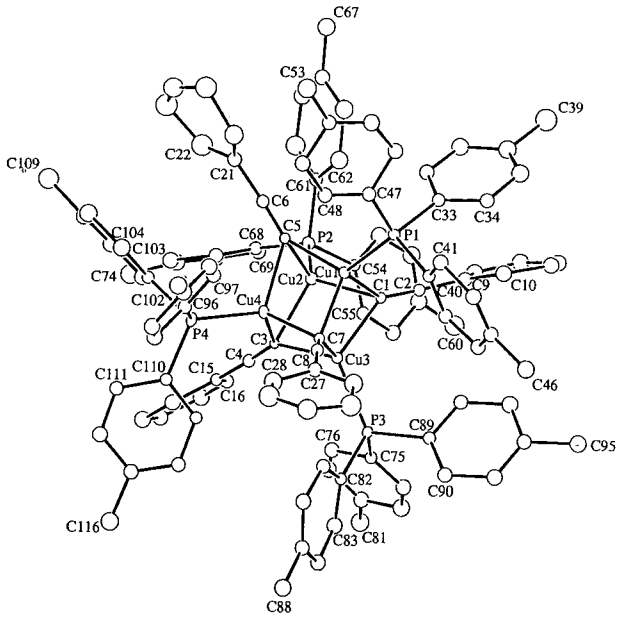

Fig. 3. The perspective view of complex **5g**.

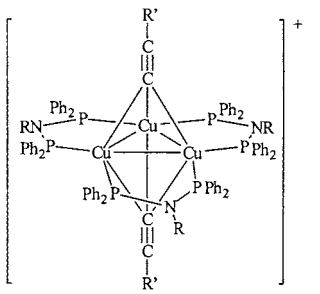

4a: R = $CH_2CH_2CH_3$, R' = C_6H_4-OCH_2CH_3-4
4b: R = $CH_2CH_2CH_3$, R' = C_6H_4-Ph-4
4c: R = $CH_2CH_2CH_3$, R' = Ph
4d: R = $CH_2CH_2CH_3$, R' = C_6H_4-NO_2-4
4e: R = Ph, R' = C_6H_4-OCH_2CH_3-4
4f: R = Ph, R' = C_6H_4-Ph-4
4g: R = Ph, R' = Ph
4h: R = Ph, R' = $^nC_6H_{13}$
4i: R = C_6H_4-CH_3-4, R' = C_6H_4-OCH_2CH_3-4
4j: R = C_6H_4-F-4, R' = C_6H_4-Ph-4

A series of tetranuclear copper(I) acetylide complexes with monodentate phosphine ligands $[Cu_4(PR_3)_4(\mu_3\text{-}\eta^1\text{-}C{\equiv}C{-}R')_4]$ [R = Ph, R′ = C_6H_4–CH_2CH_3-4 (**5a**), C_6H_4–OCH_3-4 (**5b**), C_6H_4–Ph-4 (**5c**), C_6H_4–NO_2-4 (**5d**), Ph (**5e**); R = C_6H_4–F-4, R′ = Ph (**5f**); R = C_6H_4–CH_3-4, R′ = Ph (**5g**); R = C_6H_4–OCH_3-4, R′ = Ph (**5h**)] [14,21] have also been found to possess rich photophysical properties. The structures of some of these complexes have been studied by X-ray crystallography [14,21,34]. The perspective view of **5g** is depicted in Fig. 3. In general, the four copper(I) centres are arranged in a distorted tetrahedron with each of the four triangular faces being capped by a μ_3-η^1-acetylide ligand. Each of the copper(I) centres is also coordinated with a monodentate phosphine ligand. Alternatively, the molecular structure of these complexes can also be described as a distorted cubane structure. Although the crystal structures of some of the complexes are not available, it is reasonable to assume that the molecular structures of this class of complexes are similar based on their similar spectroscopic properties. The electronic absorption spectra of these tetranuclear copper(I) acetylide complexes show a peak at ca. 260 nm, with a shoulder at ca. 320 nm and long absorption tails extending to 500 nm. The highest energy absorption bands have been assigned as intraligand transitions. The complexes display intense and long-lived luminescence upon photoexcitation. Some of the complexes exhibit vibronically structured emission bands in the solid state and/or in low temperature glass. Progressional spacings of ca. 1360–1650 and ca. 1740–2100 cm^{-1} have been observed, which are typical of ground-state $\nu(C{\cdots}C)$ aromatic and $\nu(C{\equiv}C)$ acetylide stretching frequencies, respectively. The photophysical data are collected in Table 4. The emission spectra in CH_2Cl_2 at 298 K of the phenylacetylide complexes are very similar and display dual luminescence at ca. 420 and 620 nm. In addition, a shoulder at ca. 520 nm on the high energy side of the 620-nm band has also been observed.

Table 4
Photophysical data for **5a**–**h**

Complex	Medium (T/K)	Emission wavelength λ_{max}/nm (τ_o/μs)	Reference
5a	Solid (298)	548 (129.0)	[21]
	Solid (77)	479, 528, 582 sh	
	CH_2Cl_2 (298)	515, 668 (3.1)	
5b	Solid (298)	450, 480 (7.5, 36.0)	[21]
	Solid (77)	443, 480	
	CH_2Cl_2 (298)	672 (2.7)	
5c	Solid (298)	540 (1.3, 4.8)	[21]
	Solid (77)	537, 600 sh	
	CH_2Cl_2 (298)	508, 675 (3.1)	
5d	Solid (298)	400 (<0.1)	[21]
	Solid (77)	618, 675 sh	
	CH_2Cl_2 (298)	610 (<0.1), 665[a]	
5e	Solid (298)	483 sh (3.7 ± 0.3), 522 (3.7 ± 0.3)	[14]
	Solid (77)	477, 524	
	CH_2Cl_2 (298)	420, 520 sh (<0.01), 616 (3.6 ± 0.3)	
5f	Solid (298)	516 (1.3 ± 0.1)	[14]
	Solid (77)	516	
	CH_2Cl_2 (298)	420, 510 sh, 606 (0.86 ± 0.09)	
5g	Solid (298)	548 (0.52 ± 0.05)	[14]
	Solid (77)	535	
	CH_2Cl_2 (298)	410, 510 sh, 620	
5h	Solid (298)	529 (2.9 ± 0.3)	[14]
	Solid (77)	521	
	CH_2Cl_2 (298)	410, 670	

[a] Excitation wavelength = 530 nm.

For the complexes with PPh_3 and different acetylides as ligands, similar broad and unstructured low energy emission bands at ca. 665–675 nm are also observed.

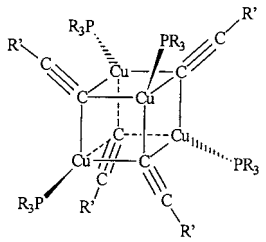

5a: R = Ph, R' = C_6H_4-CH_2CH_3-4
5b: R = Ph, R' = C_6H_4-OCH_3-4
5c: R = Ph, R' = C_6H_4-Ph-4
5d: R = Ph, R' = C_6H_4-NO_2-4
5e: R = Ph, R' = Ph
5f: R = C_6H_4-F-4, R' = Ph
5g: R = C_6H_4-CH_3-4, R' = Ph
5h: R = C_6H_4-OCH_3-4, R' = Ph.

For **5c** and **5d**, the emission bands occur at very low energies and are comparable to those of the free acetylenes. Therefore, the emission of these two cubane-type complexes has been assigned to arise from a ligand-centred π–π^*(acetylide) emissive state. Comparing the low energy emission bands of **5a**, **5b** and **5e** in CH_2Cl_2, a small red-shift in energy is observed on going from the phenylacetylide complex to the 4-alkyl- or 4-alkoxyphenylacetylide counterparts. This is in line with the σ-donating properties of the acetylide ligands. Therefore, it is likely that the emissive state of these cubane-type complexes contain some LMCT [acetylide $\rightarrow Cu_4$] character. However, based on the short Cu···Cu distances [2.5092(5)–2.6636(8) Å] [14,21,34] observed in these complexes, as well as the relatively small dependence of the emission energies on the nature of the ligands, it is likely that the excited state for the low energy emission should bear a parentage of large copper-centred (d-s) character modified by metal–metal interaction delocalized over the cluster core.

A novel tetranuclear copper(I) acetylide complex $[Cu_4(PPh_3)_4(\mu_3\text{-}\eta^1,\eta^1,\eta^2\text{-}C{\equiv}C\text{–}C_6H_4\text{–}OCH_3\text{-}4)_3]^+$ (**6**) has also been isolated from the reaction of $[Cu(CH_3CN)_4]PF_6$ with PPh_3 and $[Au(C{\equiv}C\text{–}C_6H_4\text{–}OCH_3\text{-}4)]_\infty$ in CH_2Cl_2 [15].

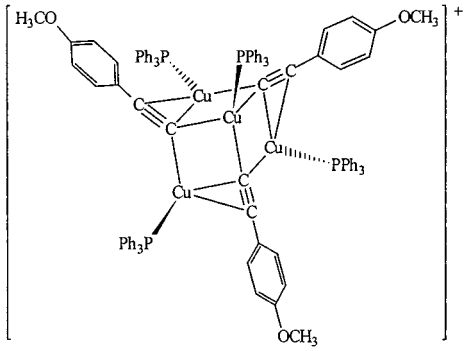

6

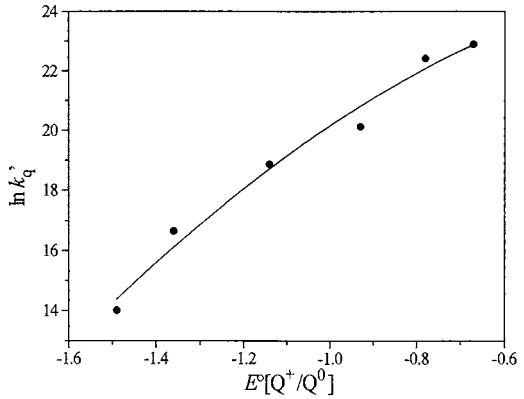

Fig. 4. A plot of ln k_q' versus $E°[Q^+/Q^0]$ for the oxidative electron-transfer quenching of **6*** by a series of structurally related pyridinium acceptors.

The crystal structure of the complex can be described as an open cube with a vertex missing. The electronic absorption spectrum of the complex shows a high energy shoulder at ca. 252 nm and a peak at ca. 330 nm. Excitation of the complex in the solid state and in fluid solutions results in long-lived intense luminescence. The solid sample shows an emission band at 445 nm and a shoulder at ca. 630 nm ($\tau_o = 20.7 \pm 1$ μs) at 298 K. The complex emits at 675 nm in acetone ($\tau_o = 4.0 \pm 0.4$ μs) and CH_2Cl_2 ($\tau_o = 2.7 \pm 0.3$ μs). In view of the short Cu···Cu distance [2.446(2) Å] and the strong σ-donating properties of the 4-methoxyphenylacetylide ligand, the low energy emission of the complex has been assigned to originate from a ^{3}LMCT [acetylide $\rightarrow Cu_4$] excited state mixed with a metal-centred d-s state modified by copper–copper interactions. The phosphorescent state of **6** has also been found to undergo facile electron transfer reactions with a series of structurally related pyridinium acceptors. An excited-state reduction potential $E°[Cu_4^{2+}/Cu_4^{+}*]$ of -1.71 V ($\lambda = 1.36$ eV) versus SSCE has been estimated for **6*** by a three-parameter, non-linear least-squares fit to the equation:

$$(RT/F)\ \ln k_q' = (RT/F)\ \ln K\kappa\nu - (\lambda/4)[1 + (\Delta G°'/\lambda)]^2$$

where k_q' is the bimolecular quenching rate constants corrected for diffusional effects, $\Delta G°' = E°[Cu_4^{2+}/Cu_4^{+}*] - E°[Q^+/Q^0] + \omega_p - \omega_r$, where $E°[Q^+/Q^0]$ is the reduction potential of the pyridinium acceptors Q^+, ω_p and ω_r are the respective coulombic work terms to separate the products and to bring the reactants together, $K = k_D/k_{-D}$, κ is the transmission coefficient, ν is the nuclear frequency, and λ is the reorganization energy for electron transfer. A plot of ln k_q' versus $E°[Q^+/Q^0]$ for the oxidative electron-transfer quenching is depicted in Fig. 4. The close agreement between the theoretical curve and the experimental data suggests that the mechanism of the photoreactions is outer-sphere electron-transfer in nature. The highly negative

reduction potential is indicative of the strongly reducing properties of the excited complex.

In an attempt to build higher oligomers employing a trinuclear copper(I) trimethylsilylacetylide $[Cu_3(\mu\text{-dppm})_3(\mu_3\text{-}\eta^1\text{-}C{\equiv}C{-}SiMe_3)_2]^+$ as the precursor complex, reaction of $[Cu_2(\mu\text{-dppm})_2(CH_3CN)_2]^{2+}$ with trimethylsilylacetylene and *n*-butyllithium in THF gave a novel tetranuclear copper(I) acetylide complex $[Cu_4(\mu\text{-dppm})_4(\mu_4\text{-}\eta^1,\eta^2\text{-}C{\equiv}C)]^{2+}$ (**7**) [16].

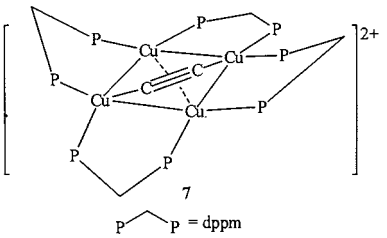

7

P P = dppm

The perspective view of the complex cation of **7** is illustrated in Fig. 5. X-ray crystallographic studies reveal that the complex exhibits a crystallographic C_2 symmetry, with the four copper(I) centres arranged in a distorted rectangular array and the four dppm ligands bridging each of the four Cu–Cu edges in a saddle-like arrangement. The most remarkable feature is the presence of an acetylido ligand bridging the four copper(I) centres with both η^1 and η^2 bonding modes. The electronic absorption spectrum reveals a high energy intraligand (dppm) absorption band at 262 nm and a low energy absorption at ca. 374 nm which has been assigned to arise from a LMCT $[C_2^{2-} \rightarrow Cu_4]$ transition. Photoexcitation of the complex results in intense and long-lived greenish–yellow emission. The solid sample emits at 509 nm ($\tau_o = 9.8$ μs) and 551 nm at 298 and 77 K, respectively. In acetone solution, the emission occurs at 562 nm ($\tau_o = 16.0$ μs, $\Phi = 0.22$). In view of the strong σ-donating properties of the acetylide and the relatively long Cu···Cu distances [3.245(2)–3.264(2) Å], the origin of the emission has been assigned to be predominantly ^{3}LMCT $[(C{\equiv}C)^{2-} \rightarrow Cu_4]$ in nature. The phosphorescent state of this complex has also been found to be highly reducing. An excited-state reduction potential $E°[Cu_4^{3+}/Cu_4^{2+}*]$ of -1.77 V ($\lambda = 1.36$ eV) versus SSCE has been estimated for **7*** from oxidative quenching experiments with a series of structurally related pyridinium acceptors.

Apart from trinuclear and tetranuclear systems, the dinuclear copper(I) acetylide complex $[Cu_2(PPh_2CH_3)_2(\mu,\eta^1\text{-}C{\equiv}C{-}Ph)_2]$ (**8**) has also been found to possess rich photophysical properties [17].

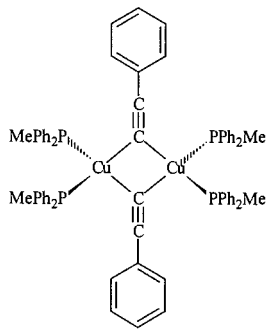

8

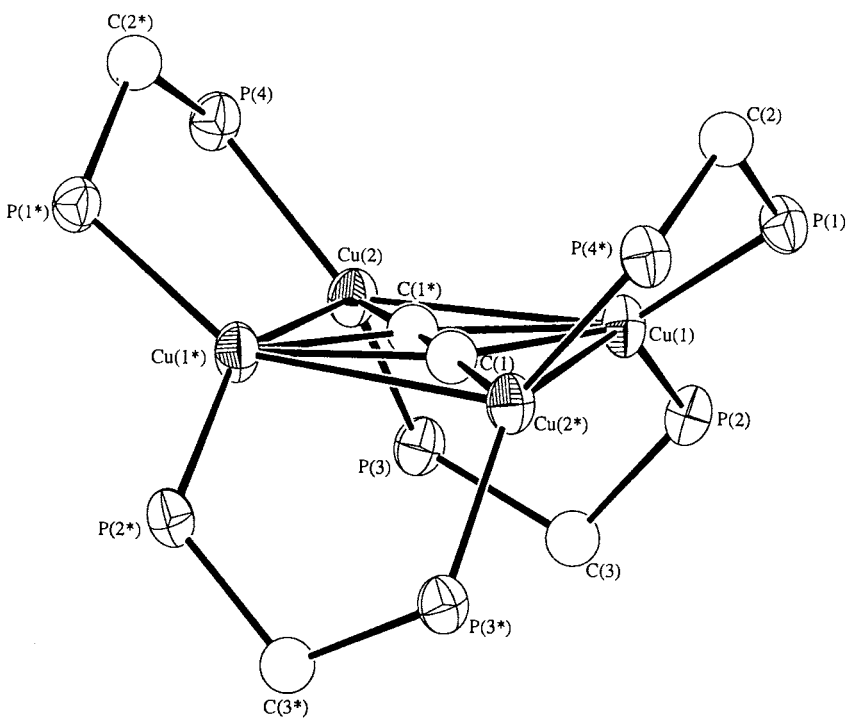

Fig. 5. The perspective view of the complex cation of **7**. Hydrogen atoms and phenyl rings have been omitted for clarity.

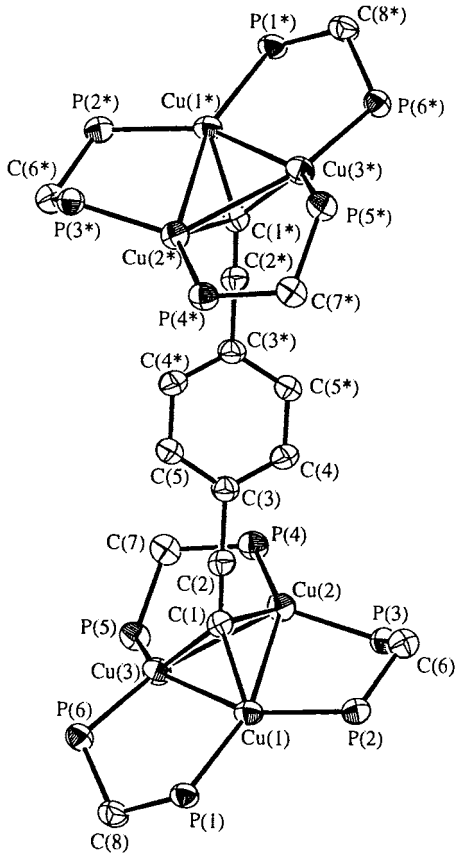

Fig. 6. The perspective view of the complex cation of **9**. Hydrogen atoms and phenyl rings have been omitted for clarity.

In CH_2Cl_2, the complex shows a strong absorption band at ca. 248 nm with a shoulder at ca. 315 nm, and a long absorption tail to lower energy. The complex is strongly luminescent in the solid state (at 298 K, $\lambda_{max} =$ 467 and 509 nm, $\tau_o = 87 \pm 5$ μs) and in fluid solutions (in CH_2Cl_2, $\lambda_{max} = 529$ and 660 nm). The 77 K solid-state emission spectrum shows a vibronically structured band with progressional spacings of ca. 1982 cm^{-1}, typical of $\nu(C \equiv C)$ stretch of the acetylide moiety as observed in the IR spectrum. Based on the strong σ-donating properties of the acetylide units, together with the short Cu···Cu distance [2.454(1) Å], the excited state responsible for the long-lived emission has been proposed to originate from a ^{3}LMCT [acetylide → Cu_2] state, probably mixed with a copper-centred (d-s) state modified by the copper–copper interaction in the dimer.

As an extension of our work on di-, tri- and tetranuclear copper(I) acetylide complexes, attempts have also been made to synthesize luminescent rigid-rod oligomers based on the triangulo-M_3 building blocks. In this context, a hexanuclear copper(I) acetylide complex $[Cu_3(\mu\text{-dppm})_3(\mu_3\text{-}\eta^1\text{-}C{\equiv}C{-}C_6H_4{-}C{\equiv}C\text{-}4)Cu_3(\mu\text{-dppm})_3]^{4+}$ (**9**) has been successfully isolated and its photophysical properties studied [19]. The perspective view of the complex cation of **9** is shown in Fig. 6. The complex contains two triangular arrays of copper centres with a dppm ligand bridging each edge to form two roughly planar Cu_3P_6 cores, which are bridged by a 1,4-diethynylbenzene unit to form a dumb-bell shaped structure. The absorption spectrum of complex **9** shows strong ligand-centred absorption bands in the UV region at ca. 258–324 nm. Vibronically structured absorption bands have also been observed at ca. 370–416 nm with progressional spacings of ca. 1475–1500 cm^{-1}, which are typical of the $\nu(C{\cdots}C)$ stretching frequencies of phenyl rings in the excited state. Complex **9** displays a long-lived intense orange–yellow emission. The photophysical data are summarized in Table 5. Both the excitation and emission spectra of the complex at 298 and 77 K show vibronically structured bands with vibrational progressions typical of $\nu(C{\cdots}C)$ stretches of the aromatic ring. This observation suggests the involvement of the highly conjugated arylacetylide ligand in the excited state properties of the complex. The excited state of the complex has been proposed to bear a substantial ^{3}LMCT (acetylide → Cu) character, and probably mixed with a metal-centred d-s triplet-state. However, owing to the highly structured emission bands and the exceptionally long lifetimes, the possibile involvement of a ligand-centred π–π* (acetylide) excited state has not been ruled out.

2.2. Silver(I) acetylides

Although there have been a number of silver(I) acetylide systems reported in the literature [6,35], the photochemistry of this class of compounds still remains comparatively unexplored. One of the reasons is the photosensitivity of many silver compounds. Owing to the similar bonding geometry of copper(I) and silver(I), isolation of related silver(I) acetylide complexes is promising and such complexes should also enable the comparison of the photophysical and photochemical behaviour of this class of acetylide complexes. The synthesis and photophysical properties of a series of trinuclear silver(I) acetylides $[Ag_3(\mu\text{-P–P})_3(\mu_3\text{-}\eta^1\text{-}C{\equiv}C{-}R)]^{2+}$ [P–P = dppm, R = Ph (**10a**), $C_6H_4{-}OCH_3$-4 (**10b**), $C_6H_4{-}NO_2$-4 (**10c**); P–P = $(Ph_2P)_2N{-}CH_2CH_2CH_3$, R = Ph (**10d**)] [36] and $[Ag_3(\mu\text{-dppm})_3(\mu_3\text{-}$

Table 5
Photophysical data for **9**[a]

Medium (T/K)	Emission wavelength λ_{max}/nm (τ_o/μs)
Solid (298)	583 (222)
Solid (77)	582
CH_2Cl_2 (298)	596 (40)
EtOH/MeOH (4:1 v:v) (77)	579

[a] Data from reference [19].

Table 6
Ag···Ag distances of selected polynuclear silver(I) acetylide complexes

Complex	Ag···Ag (Å)	Reference
$[Ag_3(\mu\text{-dppm})_3(\mu_3\text{-}\eta^1\text{-}C{\equiv}C\text{–}C_6H_4\text{–}NO_2\text{-}4)]^{2+}$ (**10c**)	2.9850(6)–3.4030(6)	[36]
$[Ag_3(\mu\text{-dppm})_3(\mu_3\text{-}\eta^1\text{-}C{\equiv}C\text{–}Ph)_2]^{+}$ (**10e**)	2.866(2)–2.983(1)	[37]
$[Ag_3(\mu\text{-dppm})_3(\mu_3\text{-}\eta^1\text{-}C{\equiv}C\text{–}C_6H_4\text{–}NO_2\text{-}4)_2]^{+}$ (**10f**)	2.8946(8)–3.1948(9)	[36]
$[Ag_3(\mu\text{-dppm})_3(\mu_3\text{-}\eta^1\text{-}C{\equiv}C\text{–}C_6H_4\text{–}C{\equiv}C\text{-}4)Ag_3(\mu\text{-dppm})_3]^{4+}$ (**11**)	3.079(1)–3.338(1)	[19]

η^1-C≡C–R)$_2$]$^+$ {R = Ph (**10e**) [37], C_6H_4–NO_2-4 (**10f**) [36]} have been reported. The structures of these complexes are analogous to the trinuclear copper(I) acetylide counterparts.

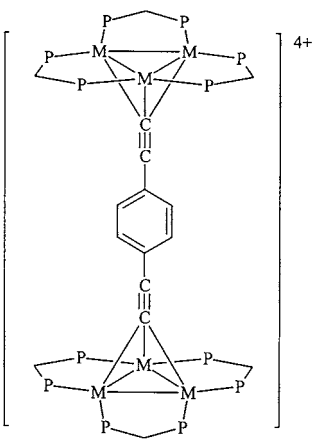

9: M = Cu
11: M = Ag

= dppm

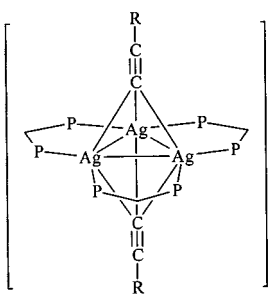

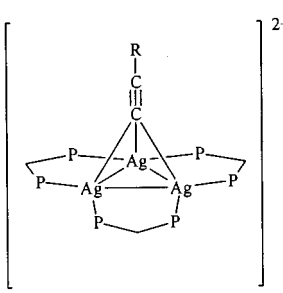

10a: R = Ph
10b: R = C_6H_4-OCH_3-4
10c: R = C_6H_4-NO_2-4

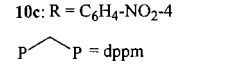

= dppm

10d: R = Ph

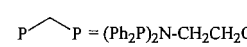

= $(Ph_2P)_2N$-$CH_2CH_2CH_3$

10e: R = Ph
10f: R = C_6H_4-NO_2-4

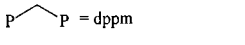

= dppm

The Ag···Ag distances range from 2.866(2) to 3.4030(6) Å (Table 6), comparable to the sum of van der Waals' radii of silver (3.44 Å) [38]. The photophysical data of these luminescent silver(I) acetylide complexes are collected in Table 7. Some of the complexes exhibit vibronically structured emission bands at both 77 and 298 K with progressional spacings of ca. 1880–2080 cm^{-1} which are attributed to the stretching frequencies of the acetylide moieties in the ground state. In some cases, additional vibrational progressions with spacings of ca. 1450–1600 cm^{-1} have also been observed, which are typical of the stretching frequencies of the aromatic rings in the ground state.

A comparison of the photophysical properties of these silver(I) acetylides with the corresponding copper(I) analogues has also been made. For example, the 77 K solid-state emission bands of **10a** and **10b** occur at ca. 0.29 and 0.33 eV higher in energy than their copper(I) counterparts **2a** and **2e**, respectively. The possibility of an MLCT [silver → π*(acetylide)] excited state is less likely in view of the large difference (1.19 eV) between the ionization energies of Cu^+ (g) and Ag^+ (g) [39]. Instead, the emission has been attributed to a ^{3}LMCT [acetylide → Ag_3] state, and probably mixed with a metal-centred (ds/dp) triplet state. However, the mixing of an intraligand π–π*(acetylide) state is also possible, in view of the highly structured emission spectra, exceptionally long lifetime and the low-lying π* orbitals of the less electron-rich acetylides.

A hexanuclear silver(I) acetylide complex $[Ag_3(\mu\text{-dppm})_3(\mu_3\text{-}\eta^1\text{-}C{\equiv}C\text{–}C_6H_4\text{–}C{\equiv}C\text{-}4)Ag_3(\mu\text{-dppm})_3]^{4+}$ (**11**) has also been isolated and its photophysical properties studied [19]. Similar to the case of the copper(I) analogue **9**, the electronic absorption spectrum of complex **11** displays strong intraligand absorption bands at ca. 258–324 nm. Apart from this, vibronically structured absorption bands have also been observed at ca. 324–364 nm with progressional spacings of ca. 1475–1500 cm^{-1}, which are typical of the ν(C≡C) stretching frequencies of the phenyl rings in the excited state. The complex shows strong and long-lived green luminescence upon photoexcitation. The photophysical data are summarized in Table 8. The solid-state emission spectra of **9** and **11** at 298 K are displayed in Fig. 7. A blue-shift in the solid-state emission energy at 77 K on going from the copper(I) complex **9** to the silver(I) complex **11** is suggestive of the presence of substantial ^{3}LMCT [acetylide → Cu/Ag] character in the excited states of the complexes, which are also probably mixed with some metal-centred d-s character. In view of a small difference (0.27 eV) in the emission energies, a MLCT [Cu/Ag → π*(acetylide)] excited state is less likely although it would give a similar energy trend. Owing to the highly structured emission bands and the

Table 7
Photophysical data for **10a–f**

Complex	Medium (T/K)	Emission wavelength λ_{max}/nm (τ_o/μs)	Reference
10a	Solid (298)	430, 449, 467, 488 sh (93.0)	[36]
	Solid (77)	428, 462, 469, 495, 515, 536 sh	
	EtOH/MeOH (4:1 v:v) (77)	432, 453, 470, 496 sh	
10b	Solid (298)	464 (5.2)	[36]
	Solid (77)	443, 464, 482, 508 sh	
	EtOH/MeOH (4:1 v:v) (77)	434, 452, 474, 494, 526 sh	
10c	Solid (298)	526, 546 sh, 615 sh (48.0)	[36]
	Solid (77)	535, 575	
	EtOH/MeOH (4:1 v:v) (77)	508, 550 sh, 600 sh	
10d	Solid (298)	512 (2.9)	[36]
	Solid (77)	553	
10e	Solid (298)	440 (0.43)	[37]
	CH_2Cl_2 (298)	440 (<0.05)	
10f	Solid (298)	570, 627 sh (<0.1)	[36]
	Solid (77)	532, 579	
	$CHCl_3$ (77)	534, 598 sh	

significantly long lifetimes, as well as the extended π-conjugation of the bridging diyne unit, an involvement of ligand-centred π–π*(acetylide) character in the lowest energy excited state is also possible.

2.3. Gold(I) acetylides

As the most common coordination geometry of gold(I) is two-coordinate (linear) and three-coordinate (trigonal planar), the molecular structures of gold(I) acetylides are usually very different from those of copper(I) and silver(I) acetylides. In addition to the common observation of short Au···Au contacts due to relativistic effects, gold(I) acetylides have been found to exhibit a wide range of molecular structures [40,41]. Recently, oligomeric and polymeric gold(I) acetylide complexes have also been focused on with increasing attention [42].

The photophysics and photochemistry of luminescent polynuclear gold(I) complexes have been extensively studied in the past decade [43–48]. The luminescence properties of organometallic gold(I) complexes have also been reported recently [49–61]. The first report on the luminescence of gold(I) acetylides appeared in 1993 in which the emissive behaviour of the complex $[Au_2(\mu\text{-dppe})_2(C{\equiv}C{-}Ph)_2]$ (**12**) was described [51].

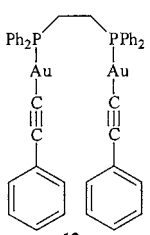

12

The X-ray crystal structure of the complex did not show any intramolecular Au···Au interaction. However, it has been found that two $[Au_2(\mu\text{-dppe})_2(C{\equiv}C{-}Ph)_2]$ units interact with each other, leading to an intermolecular Au···Au separation of 3.153(2) Å. The Au···Au distances of selected Au(I) acetylide complexes are listed in Table 9. The complex displays a ligand-centred emission at 420 nm in CH_2Cl_2 solution at 298 K. The solid sample emits at 550 nm at 298 K. This lower energy emission has been suggested by Che and coworkers to be derived from a $(d_{\delta*})^1(p_\sigma)^1$ triplet excited state, where the $d_{\delta*}$ antibonding orbitals originate from the interactions among the two $5d_{xy}$ and two $5d_{x^2-y^2}$ orbitals from two Au centres and p_σ from the interactions between the two $6p_z$ orbitals (Au–Au vector taken as the z-axis).

Reaction of $[Au(C{\equiv}C{-}Ph)]_\infty$ with dppm afforded the trinuclear complex $[Au_3(\mu\text{-dppm})_2(C{\equiv}C{-}Ph)_2]$-$[Au(C{\equiv}C{-}Ph)_2]$ (**13**) [52].

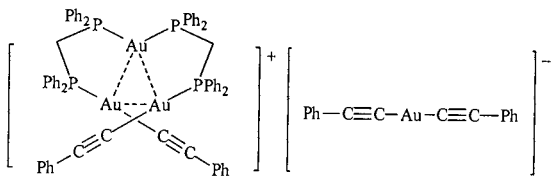

13

X-ray crystallographic studies reveal Au···Au separations of 3.167(2) and 3.083(2) Å. The complex exhibits

Table 8
Photophysical data for **11**[a]

Medium (T/K)	Emission wavelength λ_{max}/nm (τ_o/μs)
Solid (298)	513 (351)
Solid (77)	515
CH_2Cl_2 (298)	515 (426)
EtOH/MeOH (4:1 v/v) (77)	510

[a] Data from reference [19].

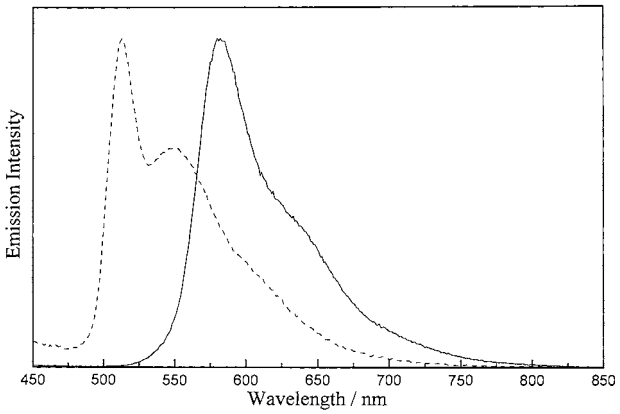

Fig. 7. The solid-state emission spectra of **9** (—) and **11** (· · ·) at 298 K.

a high energy ligand-centred π–π* (acetylide) absorption band at 276 nm ($\varepsilon = 6.9 \times 10^4$ dm^3 mol^{-1} cm^{-1}) and a lower energy intense absorption shoulder at ca. 315–375 nm ($\varepsilon = 10^4$–10^3 dm^3 mol^{-1} cm^{-1}). The low energy absorption shoulder has been tentatively suggested by Che and coworkers to be a $^1[d_{\delta*} \rightarrow p_\sigma]$ transition, and probably mixed with some intraligand character. In acetonitrile, the complex displays a high energy ligand-centred emission at 425 nm ($\tau_o = 0.45$ μs) and a low energy band at 600 nm ($\tau_o = 8.7$ μs). An emissive state of $^3[(d_{\delta*})^1(p_\sigma)^1]$ has also been proposed to be responsible for the low energy emission. A gold(I) acetylide polymer $[\{Au_2(\mu\text{-dpppy})(C{\equiv}C{-}Ph)_2\}_\infty]$ (**14**) has also been synthesized similarly by the reaction of $[Au(C{\equiv}C{-}Ph)]_\infty$ with dpppy [53].

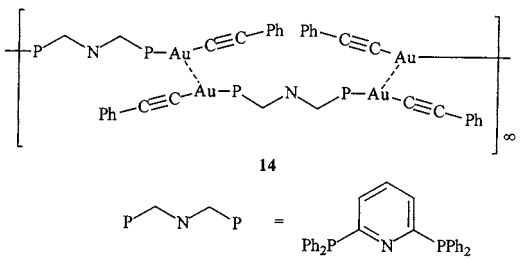

A Au···Au distance of 3.252(1) Å has been revealed by X-ray crystallographic studies. The solid sample was reported to emit at 500 nm at 77 K.

A series of gold(I) acetylides $[(C_6H_4{-}CH_3\text{-}4)_3P{-}Au{-}(BL){-}Au{-}P(C_6H_4{-}CH_3\text{-}4)_3]$ [H_2BL = 1,4-diethynylbenzene (**15a**), 9,10-diethynylanthracene (**15b**)] and $[Au_2(\mu\text{-}P{-}P)(C{\equiv}C{-}R)_2]$ (P–P = dppn, R = C_6H_4–Ph-4 (**16a**), C_6H_4–OCH_3-4 (**16b**), $^nC_6H_{13}$ (**16c**); P–P = dcpn, R = C_6H_4–Ph-4 (**17**); P–P = dmpm, R = Ph (**18a**), C_6H_4–OCH_3-4 (**18b**)] and $[Au_3(\mu_3\text{-dmmp})(C{\equiv}C{-}R)_3]$ [R = Ph (**19a**), C_6H_4–OCH_3-4 (**19b**)] with bridging phosphine or acetylide ligands have been reported by us recently [54].

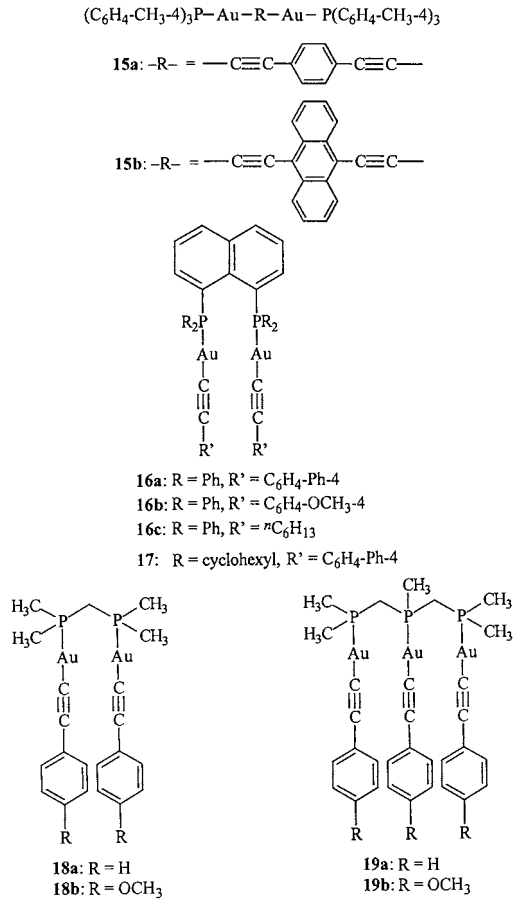

Table 9
Au···Au distances of selected polynuclear gold(I) acetylide complexes

Complex	Au···Au (Å)	Reference
$[Au_2(\mu\text{-dppe})_2(C{\equiv}C{-}Ph)_2]$ (**12**)	3.153(2)[a]	[51]
$[Au_3(\mu\text{-dppm})_2(C{\equiv}C{-}Ph)_2][Au(C{\equiv}C{-}Ph)_2]$ (**13**)	3.083(2), 3.167(2)	[52]
$[\{Au_2(\mu\text{-dpppy})(C{\equiv}C{-}Ph)_2\}_\infty]$ (**14**)	3.252(1)[a]	[53]
$[Au_4(\mu_4\text{-tppb})(C{\equiv}C{-}Ph)_4]$ (**21b**)	3.1541(4)	[55]
$[Au\{CN\text{-}C_6H_3\text{-}(CH_3)_2\text{-}2,6\}(C{\equiv}C{-}Ph)]$ (**26**)	3.329(4)[a]	[59]
$[Au_2(\mu\text{-tmb})(C{\equiv}C{-}Ph)_2]$ (**27a**)	3.565(2)[a]	[59]
$[Au_2(\mu\text{-dmb})(C{\equiv}C{-}Ph)_2]$ (**27b**)	3.485(3)	[59]
$[(CH_3)_3P{-}Au{-}C{\equiv}C\text{-}(C_6H_2{-}\{CH_3\}_2\text{-}2,5){-}C{\equiv}C{-}Au{-}P(CH_3)_3]$ (**29b**)	3.1361(9)[a]	[61]
$[\{C_6H_3{-}(CH_3)_2\text{-}2,6\}{-}N{\equiv}C{-}Au{-}C{\equiv}C{-}(C_6H_4{-}NO_2\text{-}4)]$ (**30**)	3.923[a]	[61]

[a] Intermolecular Au···Au distances.

Table 10
Photophysical data for **15a–b**, **16a–c**, **17**, **18a–b** and **19a–b**[a]

Complex	Absorption wavelength in CH_2Cl_2 λ_{max}/nm (ε/dm^3 mol^{-1}cm^{-1})	Medium (T/K)	Emission wavelength λ_{max}/nm (τ_o/μs)
15a	242 sh (70,650), 294 (29,535), 308 (62,020), 328 (86,450)	Solid (298)	533 (82 ± 2)
		Solid (77)	520
		CH_2Cl_2 (298)	489, 521 (2.5 ± 0.3)
15b	242 sh (107,375), 276 (109,185), 300 (25,920), 324 sh (7,335), 410 (19,550), 436 (48,360), 464 (65,775)	Solid (298)	580 (<0.1)
		Solid (77)	498, 528, 561
		CH_2Cl_2 (298)	479, 500, 529 (0.40 ± 0.04)
16a	309 (95,250), 394 sh (6,100)	Solid (298)	655 (6.2 ± 0.6)
		Solid (77)	571
		CH_2Cl_2 (298)	434, 704 (0.14 ± 0.01)
16b	292 (65,720), 394 sh (3,565)	Solid (298)	571 (132 ± 3)
		Solid (77)	561
		CH_2Cl_2 (298)	714 (2.3 ± 0.2)
16c	293 (74,895), 396 sh (9,825)	Solid (298)	644 (2.0 ± 0.2)
		Solid (77)	604
		CH_2Cl_2 (298)	677 sh, 704 (1.50 ± 0.15)
17	310 (77,520)	Solid (298)	707 (4.8 ± 0.5)
		Solid (77)	569
		CH_2Cl_2 (298)	753 (2.8 ± 0.3)
18a	274 (34,015), 284 (35,635), 320 sh (14,335)	Solid (298)	490 (0.42 ± 0.04)
		Solid (77)	489
		CH_2Cl_2 (298)	528 (0.46 ± 0.05)
18b	290 (35,045), 326 sh (14,195)	Solid (298)	521 (0.95 ± 0.09)
		Solid (77)	502
		CH_2Cl_2 (298)	438, 530 (3.43 ± 0.35)
19a	272 (36,060), 284 (36,330), 324 sh (16,545)	Solid (298)	538 (1.29 ± 0.13)
		Solid (77)	529
		CH_2Cl_2 (298)	539 (1.05 ± 0.10)
19b	252 sh (35,135), 290 (35,765), 332 sh (18,970)	Solid (298)	539 (1.16 ± 0.12)
		Solid (77)	524
		CH_2Cl_2 (298)	530 (0.55 ± 0.06)

[a] Data from reference [54].

The photophysical data are summarized in Table 10. Complexes **15a** and **15b** with a bridging acetylide show vibronically structured absorption bands at ca. 294–328 and 410–464 nm with progressional spacings of 1980 and 1400 cm^{-1}, respectively. The absorption bands have been proposed to arise from intraligand π–π*(acetylide) or ^{1}[σ(Au–P) → π*(acetylide)] transitions. For the dppn complexes **16a–c**, the absorption bands occur at ca. 290–310 nm and a weaker absorption at ca. 400 nm with tailing to ca. 500 nm is also observed. These absorption bands have been proposed to be ^{1}[σ(Au–P) → π*(dppn)] in origin. The dinuclear complexes with dmpm ligand (**18a–b**) and trinuclear complexes with dmmp ligand (**19a–b**) display strong absorption bands at ca. 252–290 nm, attributable to π–π*(acetylide) or [σ(Au–P) → π*(acetylide)] transitions. These complexes also exhibit absorption shoulders at ca. 320–332 nm which are absent in the mononuclear analogues. These absorption bands have been assigned to arise from a ^{1}[$d_{\sigma^*} \rightarrow p_\sigma$] transition. However, a metal–metal-bond to ligand charge-transfer MMLCT ^{1}[d_{σ^*}(Au–Au) → π*(C≡C–R)] assignment is also possible in view of the red shift in the absorption energy from the mononuclear to the trinuclear species.

The solid-state emission of **15a** appears as a vibronically structured band at ca. 533 nm, which has been assigned to originate from a ligand-centred π–π*(acetylide) or [σ(Au–P) → π*(acetylide)] triplet state. This dinuclear complex has been found to emit at a lower energy than the mononuclear species [Au(PPh_3)(C≡CPh)] (λ_{max} = 459 nm under similar conditions) [54]. This observation has been ascribed to a lower-lying π* orbital of the bridging acetylide ligand. Similarly, the solid-state emission of **15b** has been assigned to be intraligand π → π*(anthryl) or σ(Au–P) → π*(anthryl) in origin.

The solid samples of the dppn complexes **16a–c** emit at similar energy (ca. 571–655 nm). The excited state has also been suggested to be ^{3}[σ(Au–P) → π*(naphthyl)]. For complex **17**, the electron-donating cyclohexyl rings of dcpn increase the electron density of the phosphorus atoms and therefore render the σ(Au–P) electron-pair more donating. This is in accord with the observation that the dcpn complex **17** emits at a much lower energy (707 nm) compared with **16a–c**.

The solid-state emission bands of the dinuclear gold(I) acetylide complexes **18a, 18b** and trinuclear complexes **19a** and **19b** occur at 490, 521, 538 and 539 nm, respectively. Although the emission energy shows a red shift from the dimer to the trimer, it is not sensitive to the methoxy substituent on the phenylacetylide ligand. In view of this, together with the large Stokes shifts observed, the excited state has been proposed to be metal-centred $^3[(d_{\delta*})^1(p_\sigma)^1]$ in origin. The photochemical properties of these gold(I) acetylides have also been studied. For example, the phosphorescent state of **19a** has been found to be quenched by the electron acceptor 4-methoxycarbonyl-*N*-methylpyridinium ion, with a bimolecular quenching rate constant of 4.98×10^9 dm^3 mol^{-1} s^{-1}. The electron-transfer mechanism of this photoinduced reaction, as well as that between **16b*** and MV^{2+}, have been confirmed by nanosecond transient absorption spectroscopy.

The synthesis and photophysical properties of a series of dinuclear and tetranuclear gold(I) acetylide complexes $[Au_2(\mu\text{-dppb})(C{\equiv}C{-}R)_2]$ [R = $^nC_6H_{13}$ (**20a**), Ph (**20b**), $C_6H_4{-}OCH_3$-4 (**20c**)] and $[Au_4(\mu_4\text{-tppb})(C{\equiv}C{-}R)_4]$ [R = $^nC_6H_{13}$ (**21a**), Ph (**21b**), $C_6H_4{-}OCH_3$-4 (**21c**)] have also been reported by us recently [55].

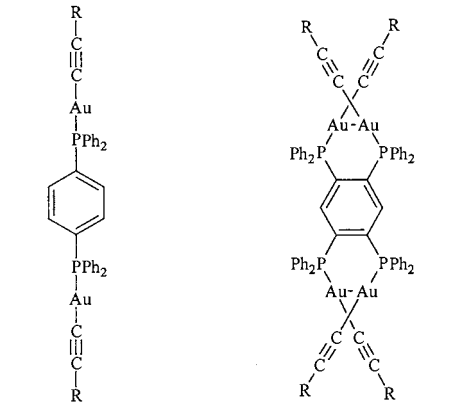

20a: R = $^nC_6H_{13}$
20b: R = Ph
20c: R = C_6H_4-OCH_3-4

21a: R = $^nC_6H_{13}$
21b: R = Ph
21c: R = C_6H_4-OCH_3-4

X-ray crystallographic studies on **21b** reveal an intramolecular Au···Au separation of 3.1541(4) Å. The perspective view of **21b** is depicted in Fig. 8. The arrangement of the two adjacent Au(C≡CPh) units is in a crossed geometry rather than a radial one. Consequently, the shape of the molecule resembles a distorted anthracene structure. The electronic absorption bands of these complexes at ca. 250–300 nm have been assigned to be $^1[\sigma(Au{-}P) \rightarrow \pi^*(Ph_{bridge})]$ transitions. The more electron-deficient 'bridging' phenyl ring of tppb relative to that of the dppb is in accord with the higher absorption energies of the dppb complexes **20a**–**c** than those of the tppb analogues **21a**–**c**. The photophysical data are listed in Table 11. In general, the methoxyphenylacetylide complexes **20c** and **21c** emit at a lower energy than the phenylacetylide counterparts **20b** and **21b**. This observation is in line with the more electron-rich methoxy moiety on the acetylide which reduces the extent of metal-to-ligand back-π-donation to the acetylide $[d\pi(Au) \rightarrow \pi^*(acetylide)]$. This leads to an increased dπ(Au)–3d(P) overlap and therefore a higher σ(Au–P) orbital energy. The photoreaction between **21c** and methyl viologen has also been studied by nanosecond transient absorption spectroscopy [54]. The transient absorption difference spectrum displays a sharp absorption band at ca. 400 nm and a broad one at ca. 600 nm, typical of the $MV^{\bullet+}$ radical absorptions. This indicates the strongly reducing properties of the phosphorescent state of **21c**. A back electron-transfer rate constant k_b of 1.94×10^{10} dm^3 mol^{-1} s^{-1} has also been estimated from a plot of $1/\Delta A$ versus time for the decay trace.

The photophysical and photochemical properties of dinuclear gold(I) acetylide complexes containing a diphosphinoferrocene bridging ligand $[Au_2(\mu\text{-dppf})(C{\equiv}C{-}R)_2]$ [R = Ph (**22a**) and ^{t}Bu (**22b**)] have also been investigated [56]. The UV–vis absorption spectra of **22a** and **22b** shows intense vibronically structured bands at ca. 270–295 nm with progressional spacings of ca. 1825 cm^{-1}, typical of ν(C≡C) stretching frequencies in the excited state.

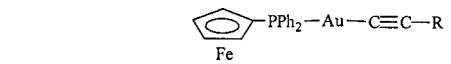

22a: R = Ph
22b: R = ^{t}Bu

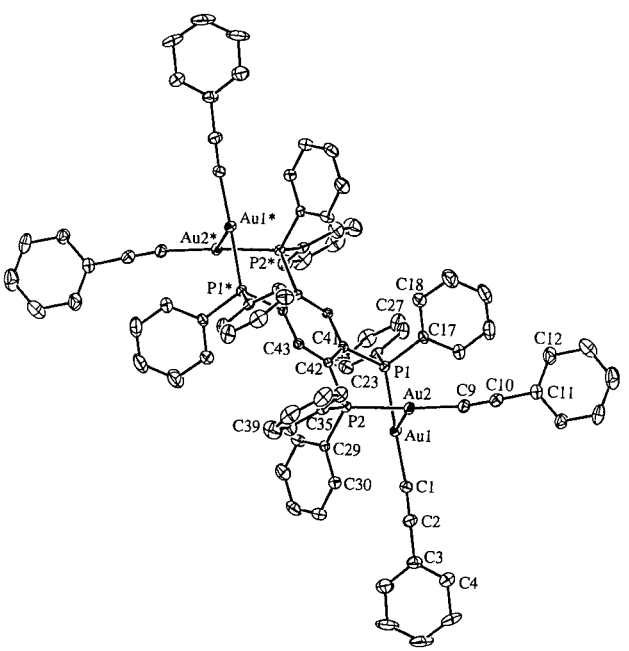

Fig. 8. The perspective view of complex **21b**. Hydrogen atoms have been omitted for clarity.

Table 11
Photophysical data for **20a-c** and **21a-c**[a]

Complex	Medium (T/K)	Emission wavelength λ_{max}/nm (τ_o/μs)[b]
20a	Solid (298)	510 (153.8)
	Solid (77)	427, 537
	CH_2Cl_2 (298)	392 (0.67); 587[c] (0.93)
20b	Solid (298)	507 (5.32)
	Solid (77)	483
	CH_2Cl_2 (298)	395, 411 sh, 476 sh, 601 sh; 628[c] (0.27)
20c	Solid (298)	486; 563[d] (5.06)
	Solid (77)	483; 556[d]
	CH_2Cl_2 (298)	395, 462 sh, 541 (2.66)
21a	Solid (298)	405, 602 (1.28)
	Solid (77)	586
	CH_2Cl_2 (298)	409, 577 (0.71)
21b	Solid (298)	599; 611[d] (0.57)
	Solid (77)	584; 611[d]
	CH_2Cl_2 (298)	510, 538 sh (0.46)
21c	Solid (298)	415; 628[d] (1.85)
	Solid (77)	414; 618[d]
	CH_2Cl_2 (298)	447, 601 (0.47)

[a] Data from reference [55].
[b] Excitation wavelength = 350 nm.
[c] Excitation wavelength = 500 nm.
[d] Excitation wavelength = 450 nm.

These absorption bands are assigned to intraligand π–π*(acetylide) transitions. The complexes are non-emissive in the solid state at 77–298 K. However, in CH_2Cl_2 solution, the complexes show weak emission bands at 410 nm. The photoreactivities of **22a** have also been studied. In CH_2Cl_2, the complex reacts with the solvent leading to the formation of the C–C coupling product Ph–C≡C–C≡C–Ph.

The photophysical properties of a number of dinuclear gold(I) complexes with bridging diacetylide ligands have also been investigated by Che and coworkers. The complex $[(C_6H_4\text{–}OCH_3\text{-}4)_3P\text{–}Au\text{–}C{\equiv}C\text{–}Au\text{–}P(C_6H_4\text{–}OCH_3\text{-}4)_3]$ (**23**) reveals vibronically structured emission band at 400–500 nm with progressional spacings of ca. 2100 cm^{-1} [57]. The emissive state has been assigned to be intraligand π–π*(acetylide) in origin.

The luminescence properties of the complexes $[(Ph)_n(Np)_{3-n}P\text{–}Au\text{–}C{\equiv}C\text{–}Au\text{–}P(Ph)_n(Np)_{3-n}]$ [n = 0–3 (**24a**–**d**)] and $[Fc_2PhP\text{–}Au\text{–}C{\equiv}C\text{–}Au\text{–}PPhFc_2]$ (**25**) have also been reported recently by Mingos and Yam [58]. Complexes **24a**–**d** show vibronically structured bands at 296 nm which have been assigned as $^1[\sigma(Au\text{–}P) \rightarrow \pi^*(Np)]$ transitions.

$(C_6H_4\text{-}OCH_3\text{-}4)_3P\text{–}Au\text{—}C{\equiv}C\text{–}Au\text{–}P(C_6H_4\text{-}OCH_3\text{-}4)_3$

23

$(Ph)_n(Np)_{3-n}P\text{–}Au\text{—}C{\equiv}C\text{–}Au\text{–}P(Ph)_n(Np)_{3-n}$

24a: n = 0
24b: n = 1
24c: n = 2
24d: n = 3

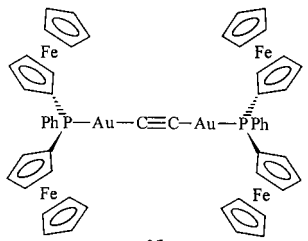

25

The solid-state emission energies of the complexes at 77 K follow the order: **24d** (523 nm) > **24c** (547 nm) > **24b** (556 nm) ≃ **24a** (554 nm), which is in line with the electron-richness around the Au–P bonds and a $^3[\sigma(Au\text{–}P) \rightarrow \pi^*(Np)]$ excited state has been proposed. The ferrocene-containing complex **25** is weakly emissive owing to the effective intramolecular reductive electron-transfer quenching by the ferrocene moiety.

The photophysical properties of luminescent gold(I) acetylides with isocyanide ligands $[Au\{CN\text{–}C_6H_3\text{–}(CH_3)_2\text{-}2,6\}(C{\equiv}C\text{–}Ph)]$ (**26**) and $[Au_2(\mu\text{-}L)(C{\equiv}C\text{–}Ph)_2]$ [L = tmb (**27a**), dmb (**27b**)] have also been reported [59].

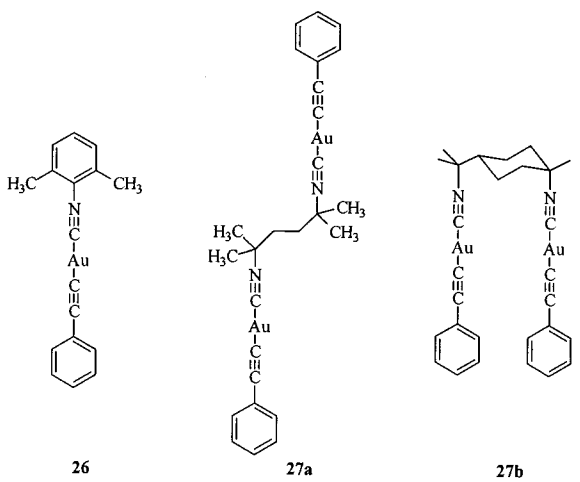

26 **27a** **27b**

X-ray crystallographic studies reveal an intermolecular Au···Au separation of 3.329(4) Å for the mononuclear complex **26**. Although **27a** is in an *anti*-configuration, an intermolecular Au···Au distance of 3.565(2) Å has been observed. The intramolecular Au···Au contact for **27b** has been found to be 3.485(3) Å. These figures suggest some very weak Au···Au interaction existing in these complexes. The complexes display intense MLCT $^1[d_{z^2} \rightarrow \pi^*(isocyanide)]$ absorption bands at ca. 240 nm. Lower energy absorption bands at ca. 273 and 288 nm are typical of intraligand π–π*(acetylide) transitions. The complexes show a structured ligand-centred π–

π*(acetylide) emission band at ca. 420 nm. However, the solid-state emission spectra of the complexes at room temperature reveal a broad band at ca. 550 nm which has been assigned to be derived from a metal-centred $^3[(d_{\delta*})^1(p_\sigma)^1]$ excited state.

A tetranuclear gold(I) phenylacetylide complex $[Au_4(\mu_4\text{-dptact})(C{\equiv}C{-}Ph)_4]$ (**28**) containing a tetraaza-macrocycle cavity has also been described by Che and coworkers [60].

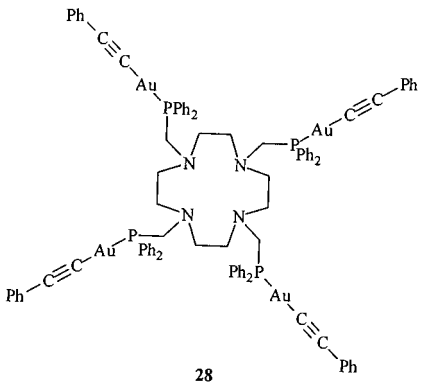

28

The electronic absorption spectrum shows an intraligand π–π*(acetylide) absorption at ca. 260–310 nm. The emission spectrum of the complex in CH_2Cl_2 solution at room temperature shows a ligand-centred emission band at ca. 425 nm and a lower energy band at 560 nm which has been suggested to be associated with the stacking of Au–C≡C–Ph units in solution. In the presence of alkali metal ions, the high energy emission is strongly enhanced. It has been suggested that inter- and/or intramolecular interactions between the Au(C≡C–Ph) moieties, which provide facile non-radiative decay pathway for the intraligand excited state, are likely to be prohibited in the presence of alkali metal ions. In the presence of Cu^+ or Ag^+, the emission at ca. 550–600 nm has been found to be enhanced.

The photoluminescence properties of a series of gold(I) acetylides with the formula $[\{-Au-C{\equiv}C-Ar-C{\equiv}C-Au-L-\}_n]$ where L = diphosphine or bis(isocyanide) have been reported recently [61]. The complexes $[(CH_3)_3P-Au-C{\equiv}C-(C_6H_2-R_2\text{-}2,5)-C{\equiv}C-Au-P(CH_3)_3]$ [R = H (**29a**), CH_3 (**29b**)] in CH_2Cl_2 emit at ca. 415 nm, attributable to a π–π*(acetylide)/[σ(Au–P) → π*(acetylide)] state. In the solid state, both complexes show an emission band at ca. 540 nm. In view of the short intermolecular Au···Au separation [3.1361(9) Å] observed in **29b**, a metal-centred $^3[(d_{\delta*})^1(p_\sigma)^1]$ excited state has been suggested to account for the red shift in emission energy. The complex $[\{C_6H_3-(CH_3)_2\text{-}2,6\}-N{\equiv}C-Au-C{\equiv}C-(C_6H_4-NO_2\text{-}4)]$ (**30**) emits at 633 nm in the solid state and at 503 nm in CH_2Cl_2 solution.

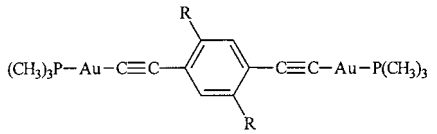

29a: R = H
29b: R = CH_3

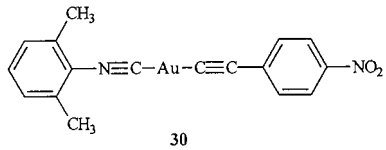

30

The occurrence of such a low energy emission has been ascribed to the electron-withdrawing NO_2 group, which stabilizes the π* orbital of the acetylide. The intermolecular Au···Au separation (3.923 Å) is too long to justify any Au···Au interactions. Instead, the stacking interactions between the phenyl rings of the acetylide and the isocyanide of two closest molecules have been suggested to give rise to the exceptionally low solid-state emission energy.

3. Rhenium(I) acetylides

The synthesis, molecular structures and chemistry of rhenium(I) acetylide complexes have been focused with a lot of attention. Beck and coworkers reported the synthesis, molecular and electronic structures of mononuclear and dinuclear pentacarbonylrhenium(I) acetylide complexes $[Re(CO)_5(C{\equiv}C-R)]$ (R = CH_3, $SiMe_3$, H) and $[(CO)_5Re-C{\equiv}C-Re(CO)_5]$ [62–64]. Besides, reactions of these complexes with other transition metal centres with different coordination geometries have also been studied [64,65]. In addition, the synthesis of rhenium(I) poly-yne complexes such as $[Re(Cp)(NO)(PPh_3)\{(C{\equiv}C)_nR\}]$ (R = CH_3, $SiMe_3$, H, Ph, 1-naphthyl, $n = 1–5$) and $[(Cp)(NO)(PPh_3)\text{-}Re(C{\equiv}C)_nRe(Cp)(NO)(PPh_3)]$ ($n = 2$, 4, 6, 8, 10), have also been reported by Gladysz and coworkers [66–74]. The chemical properties and the electrochemical behaviour of these complexes and the mixed-metal systems prepared from such complexes with terminal acetylides have also been studied in detail [71,72,74–76]. Furthermore, the synthesis and molecular structures of metal clusters containing rhenium(I) acetylide units have also been reported [77–80].

On the other hand, the photoluminescence properties of tricarbonylrhenium(I) α,α′-diimine complexes have also been extensively studied. The first report on the luminescence behaviour of rhenium(I) α,α′-diimines appeared in 1974 in which the photophysical properties of $[Re(CO)_3(phen)Cl]$ were described and a metal-to-ligand charge-transfer (MLCT) excited state assignment was proposed by Wrighton and coworkers [81]. The potential use of rhenium(I) α,α′-diimine complexes as building blocks for luminescent and redox-active

supramolecular systems has also been receiving a lot of attention [82–84]. The photophysical properties associated with the MLCT excited state of these complexes have also been shown to be highly sensitive to the nature of the environment [81–91]. Employing luminescent rhenium(I) complexes as photoswitchable materials [92,93], DNA probes and photocleavage agents [94–96], spectrochemical and luminescent probes for metal cations [97,98] as well as receptors for sugar molecules [99] has also been demonstrated by us and others recently.

In view of the well documented MLCT excited state chemistry of rhenium(I) α,α′-diimine complexes, together with the interesting structural characteristics of rhenium(I) acetylides, the photophysical and photochemical studies of mononuclear and polynuclear luminescent organometallic rhenium(I) α,α′-diimines, especially those containing an acetylide moiety, should represent a challenging area of research. In addition, incorporation of strong σ-donating acetylide ligands would raise the energy of the d–d states of the rhenium(I) centre and thereby improve the population of the MLCT state.

The luminescence properties of rhenium(I) acetylide complexes were first reported by us in 1995 [100]. A series of mononuclear rhenium(I) acetylides, $[Re(CO)_3(^tBu_2bpy)(C{\equiv}CR)]$ [R = ^{t}Bu (**31a**), $SiMe_3$ (**31b**), Ph (**31c**), $C_6H_4{-}OCH_3$-4 (**31d**), $C_6H_4{-}CH_2CH_3$-4 (**31e**), C_6H_4–Ph-4 (**31f**), 4-pyridyl (**31g**), $C_6H_4{-}C{\equiv}CH$-4 (**31h**), $^nC_6H_{13}$ (**31i**), $^nC_8H_{17}$ (**31j**), $^nC_{10}H_{21}$ (**31k**), H (**31l**)], have been synthesized, characterized and their photophysical properties studied [100,101].

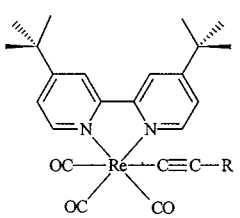

31a: R = ^{t}Bu
31b: R = $SiMe_3$
31c: R = Ph
31d: R = C_6H_4-OCH_3-4
31e: R = C_6H_4-CH_2CH_3-4
31f: R = C_6H_4-Ph-4
31g: R = 4-pyridyl
31h: R = C_6H_4-C ≡ CH-4
31i: R = $^nC_6H_{13}$
31j: R = $^nC_8H_{17}$
31k: R = $^nC_{10}H_{21}$
31l: R = H

In general, the electronic absorption spectra of these complexes in acetone show an intense low energy absorption band at ca. 391–440 nm (Table 12). With reference to related rhenium(I) α,α′-diimine systems [81–91], this absorption band has been assigned to arise from a MLCT [dπ(Re) → π*(^{t}Bu$_2$bpy)] transition. A red shift of this MLCT absorption band relative to that of the chloro counterpart [Re(CO)$_3$(^{t}Bu$_2$bpy)Cl] has been observed. This finding has been ascribed to a more electron-rich rhenium(I) centre in the acetylide complexes as a result of the stronger σ-donating ability of the acetylides than the chloro ligand. The MLCT absorption energies have also been found to follow the order: **31k** ≃ **31j** ≃ **31i** < **31a** ≃ **31d** ≃ **31e** ≃ **31c** < **31b** < **31λ**. This is in line with the σ-donating ability of the acetylides: $-C{\equiv}C{-}{}^nC_{10}H_{21}$ ≃ $-C{\equiv}C{-}{}^nC_8H_{17}$ ≃ $-C{\equiv}C{-}{}^nC_6H_{13}$ > $-C{\equiv}C{-}{}^t$Bu ≥ $-C{\equiv}C{-}C_6H_4{-}OCH_3$-4 ≃ $-C{\equiv}C{-}C_6H_4{-}CH_2CH_3$-4 > $-C{\equiv}C{-}$Ph > $-C{\equiv}C{-}SiMe_3$ > $-C{\equiv}C{-}$H. This is also in agreement with the fact that a more electron-donating acetylide would render the rhenium(I) centre more electron-rich and thereby decrease the MLCT transition energy. Similar observations have also been reported in the photoelectron spectroscopic studies of the $[FeCp(CO)_2(C{\equiv}C{-}R)]$ (R = H, Ph, ^{t}Bu) [102,103] and $[W(\equiv CH)(dmpe)_2X]$ (X = C≡C–Ph, C≡C–$SiMe_3$, C≡C–H) systems [104]. This low energy absorption of the rhenium(I) acetylides is also sensitive to the polarity of the solvent. For example, the absorption wavelength of **31a** in MeOH at 391 nm is red-shifted to 464 nm in *n*-hexane. This further supports the MLCT assignment of the low energy absorption as similar solvatochromic shifts are commonly observed for rhenium(I) α,α′-diimine complexes [86,89].

Upon photoexcitation, these mononuclear rhenium(I) acetylide complexes show intense and long-lived orange–red luminescence in the solid state and in fluid solutions. Unlike other rhenium(I) alkyl or aryl complexes which only emit at low temperature [91,105,106], this series of rhenium(I) acetylide complexes are emissive in fluid solutions at room temperature. The photophysical data are listed in Table 12. With reference to other luminescent rhenium(I) α,α′-diimine systems [81–91], the origin of the emission has been ascribed to a ^{3}MLCT [dπ(Re) → π*(^{t}Bu$_2$bpy)] excited state. The emission of the rhenium(I) acetylide complexes has also been found to occur at a lower energy relative to that of [Re(CO)$_3$(^{t}Bu$_2$bpy)Cl]. Besides, the MLCT emission energies of the rhenium(I) α,α′-diimine complexes with different acetylide ligands also show a similar trend as observed in the electronic absorption spectra. In general, more electron-donating acetylides give a lower energy MLCT emission band and this is consistent with the σ-donating ability of the acetylide moieties. However, unlike other rhenium(I) α,α′-diimine complexes whose luminescence properties are strongly dependent on the solvent [82–88,90,91,107], the emission energies of these rhenium(I) acetylides are not very sensitive to the solvent polarity. On the other hand, these luminescent rhenium(I) acetylides have also been found to exhibit interesting rigidochromism. For example, the orange–red emissions of **31i** (λ_{em} = 690 nm) and **31l** (λ_{em} = 660 nm) in a EtOH/MeOH (4:1, v:v) at 298 K are blue-shifted to λ_{em} = 560 and 545 nm for **31i** and

31l, respectively, in the 77-K glass of the same solvent mixture. Such luminescence rigidochromism has also been reported in other Re(I) α,α′-diimine systems [89].

In addition, rhenium(I) acetylide complexes with a 2,2′-bipyridine ligand [$Re(CO)_3(bpy)(C{\equiv}C{-}R)$] [R = Ph (**32a**), $C_6H_4C{\equiv}CH$-4 (**32b**)] have also been synthesized and their photophysical properties studied [108].

Table 12
Photophysical data for **31a–l**[a]

Complex	Medium (T/K)	Absorption wavelength λ_{max}/nm (ε/dm^3 mol^{-1} cm^{-1})	Emission wavelength λ_{max}/nm (τ_o/μs)
31a	MeOH (298)	275 sh (10,610), 292 (12,940), 391 (2,370)	690 (<0.1)
	Me_2CO (298)	402 (3,510)	690 (<0.1)
	CH_2Cl_2 (298)	297 (15,500), 410 (2,500)	640 (<0.1)
	THF (298)	300 sh (20,765), 328 sh (3,040), 421 (3,480)	700 (0.13)
	PhMe (298)	301 (17,630), 439 (2,740)	690 (<0.1)
	Solid (298)		610 (0.11)
	Solid (77)		610
31b	THF (298)	296 sh (21,060), 406 (3,550)	670 (0.25)
	Solid (298)		610 (0.35)
	Solid (77)		600
31c	THF (298)	325 sh (11,550), 419 (3,485)	688 (0.20)
	Solid (298)		600 (0.24)
	Solid (77)		585
31d	THF (298)	338 sh (6,620), 420 (2,290)	720 (<0.1)
	Solid (298)		600 (0.15)
	Solid (77)		585
31e	THF (298)	266 (23,725), 290 (24,700), 330 sh (8,080), 418 (3,160)	700 (<0.1)
	Solid (298)		590 (0.23)
	Solid (77)		580
31f	Me_2CO (298)	396 sh (2,860)	680 (<0.1)
	THF (298)	310 sh (36,680), 338 (25,850), 406 (2,780)	680 (<0.1)
	Solid (298)		590 (0.27)
	Solid (77)		572
31g	Me_2CO (298)	384 (3,620)	670 (<0.1)
	Solid (298)		600 (0.23)
	Solid (77)		580
31h	CH_2Cl_2 (298)	258 sh (18,505), 298 (29,170), 332 sh (16,780), 406 (2,770)	610 (<0.1)
	Solid (298)		600 (0.20)
	Solid (77)		585
31i	Me_2CO (298)	406 (2,260)	690 (<0.1)
	THF (298)	268 (47,550), 292 (54,100), 424 (3,570)	690 (<0.1)
	Et_2O (298)	258 sh (23,235), 298 (22,080), 346 sh (2,780), 440 (3,310)	680 (<0.1)
	EtOH/MeOH (4:1 v:v) (298)	250 sh (21,640), 278 sh (16,310), 296 (19,520), 404 (3,310)	690 (<0.1)
	EtOH/MeOH (4:1 v:v) (77)		560
	Solid (298)		600 (0.17)
	Solid (77)		580
31j	THF (298)	256 (17,965), 292 (19,225), 336 sh (2,510), 424 (2,540)	690 (<0.1)
	Solid (298)		580 (0.13)
	Solid (77)		570
31k	THF (298)	256 (16,990), 298 (16,990), 334 sh (3,360), 424 (2,770)	680 (<0.1)
	Solid (298)		580 (0.14)
	Solid (77)		560
31l	Me_2CO (298)	388 (3,140)	680 (< 0.1)
	CH_2Cl_2 (298)	273 (13,030), 292 (15,520), 398 (2,880)	660 (<0.1)
	THF (298)	298 sh (14,530), 404 (2,900)	670 (<0.1)
	Et_2O (298)	274 sh (13,110), 294 (17,710), 330 sh (3,131), 418 (3,050)	670 (0.25)
	EtOH/MeOH (4:1 v:v) (298)	272 sh (12,880), 292 (15,150), 386 (2,730)	660 (0.10)
	EtOH/MeOH (4:1 v:v) (77)		545
	Solid (298)		610 (0.25)
	Solid (77)		590

[a] Data from references [100] and [101].

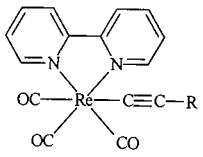

32a: R = Ph
32b: R = C_6H_4-C≡CH-4

It has been found that both the absorption and emission of the 2,2′-bipyridine counterparts occur at a lower energy than the ^{t}Bu$_2$bpy analogues with the same acetylide ligand. This observation further supports the involvement of the π* orbital of the α,α′-diimine ligands in the MLCT excited state of the complexes while the possibility of a MLCT [dπ(Re) → π*(C≡C)] excited state has been ruled out as an opposite trend in the absorption and emission energies would be observed.

In view of the growing interest in the unique physical and chemical properties of C_n-bridged metal-containing materials [62–74], diyne and poly-yne moieties represent attractive ligands to be incorporated into rhenium(I) α,α′-diimine complexes. Recently, mononuclear luminescent rhenium(I) α,α′-diimine complexes containing a diynyl moiety [Re(CO)$_3$(^{t}Bu$_2$bpy)(C≡C–C≡C–H)] (**33a**) and [Re(CO)$_3$(^{t}Bu$_2$bpy)(C≡C–C≡C–Ph)] (**33b**) have also been synthesized and characterized in our laboratory [109].

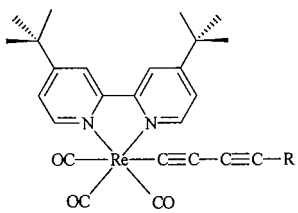

33a: R = H
33b: R = Ph

In THF, complexes **33a** and **33b** show intense absorption bands at ca. 404 and 416 nm, respectively, which have been assigned as spin-allowed MLCT [dπ(Re) → π*(^{t}Bu$_2$bpy)] transitions. The MLCT absorption of **33a** at a higher energy than that of **33b** has been rationalized by the higher Re dπ orbital energy in the latter as a result of the better σ- and π-donating abilities of C≡C–C≡C–Ph than C≡C–C≡C–H [102–104,110]. Both complexes exhibit strong orange luminescence in the solid state and in fluid solutions upon photoexcitation. The emission has also been suggested to arise from a ^{3}MLCT [dπ(Re) → π*(^{t}Bu$_2$bpy)] excited state. The MLCT emission energy of **33a** (620 nm) in THF is slightly higher than that of **33b** (625 nm). This can be accounted for by the stronger σ- and π-donating abilities of the phenyldiynyl unit than the butadiynyl ligand. Besides, the observation that both **33a** and **33b** emit at higher energies than their monoacetylide counterparts (**31l** and **31c**, respectively) excludes the possibility of a ^{3}MLCT [dπ(Re) → π*(C≡C–C≡C–R)] or a metal-perturbed ^{3}IL [π(C≡C–C≡C–R) → π*(C≡C–C≡C–R)] excited state as a reverse trend would be observed. Since the σ-donating abilities of the monoacetylide and the diynyl units are similar [102,103], such a blue-shift of emission energy from the monoacetylide to the diynyl complexes has been attributed to the much better π-accepting ability of C≡C–C≡C–R than C≡C–R, which stabilizes the rhenium(I) dπ orbitals and increases the ^{3}MLCT [dπ(Re) → π*(^{t}Bu$_2$bpy)] emission energy.

Dinuclear rhenium(I) α,α′-diimine complexes with a bridging acetylide ligand [(^{t}Bu$_2$bpy)(CO)$_3$Re–C≡C–C≡C–Re(CO)$_3$(^{t}Bu$_2$bpy)] (**34a**) [100] and [(^{t}Bu$_2$bpy)(CO)$_3$Re–C≡C–C$_6$H$_4$–(C≡C-4)–C≡C–C$_6$H$_4$–(C≡C-4)–Re(CO)$_3$(^{t}Bu$_2$bpy)] (**34b**) have also been synthesized and their photophysical properties studied.

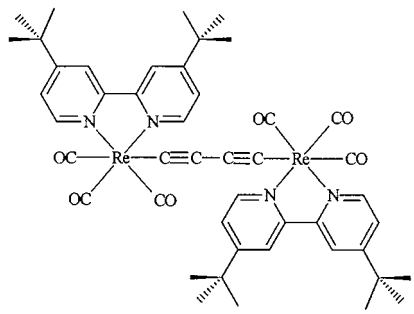

34a

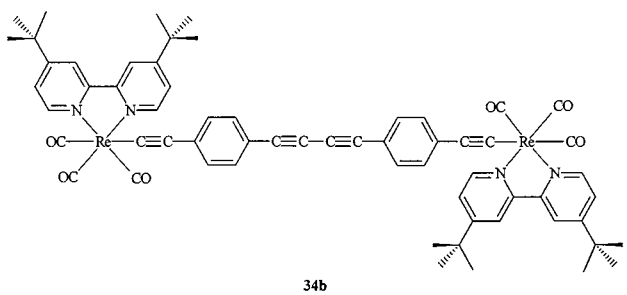

34b

The perspective view of **34a** is depicted in Fig. 9. Upon photoexcitation, complex **34a** exhibits long-lived luminescence at ca. 660–690 nm which has been proposed to originate from a ^{3}MLCT [dπ(Re) → π*(^{t}Bu$_2$bpy)] excited state. Upon excitation at $\lambda > 430$ nm, complex **34b** emits at ca. 640 nm which is at a slightly higher energy than that of the mononuclear counterpart **31h** ($\lambda_{em} = 670$ nm). The solid-state emission spectra of **34b** at 298 and 77 K show vibronically structured emission band with vibrational progressional spacings of ca. 1500 and 2000 cm^{-1}, typical of ground-state aromatic ν(C···C) and acetylide ν(C≡C) stretching frequencies, respectively.

4. Platinum(II) acetylides

The observation of luminescence from a number of platinum(II) complexes has led to an increasing interest in the design and development of luminescent materials

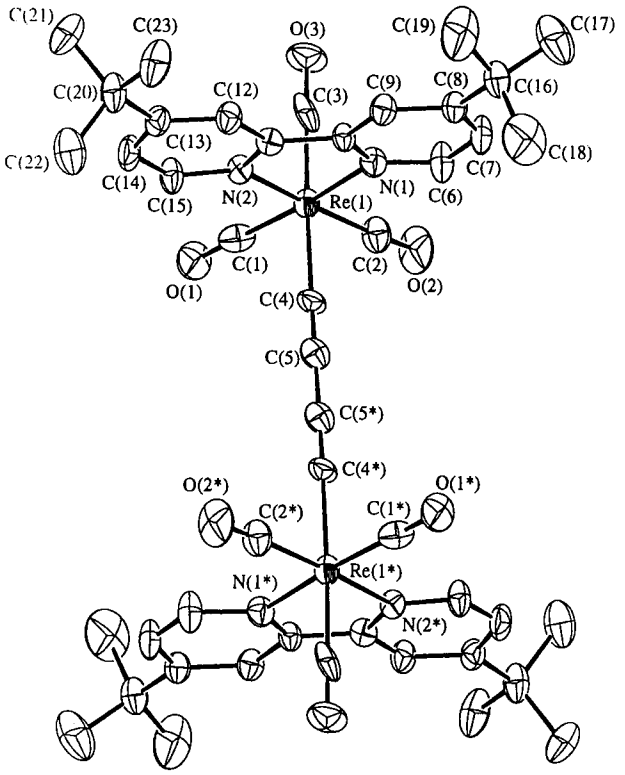

Fig. 9. The perspective view of complex **34a**. Hydrogen atoms have been omitted for clarity.

based on platinum metal centres, particularly those containing the dinuclear Pt(II) core after the discovery of the famous brightly luminescent $[Pt_2(P_2O_5H_2)_4]^{4-}$ [111–114].

The first report on the luminescence of platinum(II) complexes containing an acetylide ligand dates back to 1989 in which a dinuclear platinum(II) phenylethenylidene complex $[Pt_2(\mu\text{-}C{=}CHPh)(C{\equiv}CPh)(PEt_3)_3Cl]$ was found to exhibit red–orange luminescence in a 4:1 v/v ethanol/methanol glass at 77 K [115]. Initially Demas and coworkers attributed the observed emission to originate from a spin-forbidden metal-centred d-p phosphorescence based on the similarity of the emission to the d-p phosphorescence of Pt d^8–d^8 and d^{10}–d^{10} complexes [111–114,116,117] as well as the similarity in the splitting between the spin-allowed d-p absorption and the emission (11300 cm^{-1}) to that of dinuclear Rh(I) phosphines and arsines [118]. In a later report they reassigned the emission as derived from a spin-forbidden Pt_2-to-alkenylidene charge transfer transition [119]. The acetylide ligand was not directly involved in the lowest lying excited state although it may perturb the excited state properties through subtle electronic effects on the energy of the platinum atoms.

DeGraff, Lukehart, Demas and coworkers reported the site-selective luminescence of mononuclear Pt(II) acetylides [120]. The complexes *trans*-$[Pt(C{\equiv}CH)_2(PEt_3)_2]$ and *trans*-$[Pt(C{\equiv}CPh)_2(PEt_3)_2]$ were found to give intense vibronically structured emission in rigid glasses at 77 K. The observation of vibrational progressions in $\nu(C{\equiv}C)$ mode in the emission spectra of *trans*-$[Pt(C{\equiv}CH)_2(PEt_3)_2]$ and *trans*-$[Pt(C{\equiv}CPh)_2(PEt_3)_2]$ and additional progressions arising from phenyl-localized modes in the latter, together with the nonemissive nature of the parent *cis*- and *trans*-$[PtCl_2(PEt_3)_2]$, have prompted the authors to assign the emissive state as $Pt \rightarrow \pi^*(C{\equiv}C)$ MLCT in character upon excitation into the low-energy MLCT absorption bands. Similar assignments of the absorption bands in an extensive series of *trans*-$[M(C{\equiv}CR)_2L_2]$ (M = Ni, Pd, Pt) were reported by Masai and coworkers [121], in which the lowest-lying band was believed to arise from a transition between the $\pi(C{\equiv}CR)$ and $\pi^*(C{\equiv}CR)$ orbitals with large charge-transfer character resulting from the mixing of the $\pi^*(C{\equiv}CR)$ and the metal $(n+1)p$ orbitals.

Similar vibronically structured luminescence has also been reported for a related *trans*-$[Pt(C{\equiv}CPh)_2(dppm\text{-}P)_2]$ in 4:1 v/v ethanol/methanol glass at 77 K by Che and coworkers [122]. Extended-Hückel molecular orbital calculations on the model complex *trans*-$[Pt(C{\equiv}CPh)_2(dmpm\text{-}P)_2]$ also supported an emissive state of large platinum-to-acetylide MLCT character, with substantial mixing of the π^* orbital of phenylacetylide with the $6p_z$ orbital of Pt and of the $5d_{yz}$(Pt) orbital with the $\pi(C{\equiv}CPh)$ orbitals (taking the P–Pt–P axis as the x-axis and the phenylacetylides to lie on the y-axis). A related *cis*-$[Pt(phen)(C{\equiv}CPh)_2]$ has also been reported to emit in fluid solution at room temperature, the emissive origin of which has been assigned as derived from a ^{3}MLCT $[d\pi(Pt) \rightarrow \pi^*(phen)]$ excited state [123]. The electronic absorption spectra of a series of related complexes *cis*-$[Pt(Me_2bpy)(C{\equiv}CC_6H_4\text{-}R\text{-}4)_2]$ (R = H, Me, NO_2) have been shown to display low energy absorption bands at ca. 396 nm, which was tentatively assigned as a MLCT $[d\pi(Pt) \rightarrow \pi^*(Me_2bpy)]$ transition [124].

Subsequent luminescence studies on the polymers $[Pt\{(C{\equiv}C)_m\}_2(PBu^n)_2]_n$ by Lewis, Marder, Friend and coworkers [125] also showed the presence of vibronically structured emission bands, which they attributed to originate from an alkynyl-localized π–π^* excited state. The optical absorption, photoluminescence, and photoinduced absorption of the polymers $[Pt(PR_3)_2C{\equiv}C\text{–}L\text{–}C{\equiv}C]_n$ (R = Et, ^{n}Bu; L = pyridine, phenylene, or thiophene) have been reported and a comparison with the corresponding monomers has been made [126]. The electronic absorption spectra of the polymers $[M(C{\equiv}C\text{–}R\text{–}C{\equiv}C)_2(PR'_3)_2]_n$ (M = Ni, Pd, Pt) have also been reported with spectral assignments consistent with those of the mononuclear counterparts [127–130].

Recent work by us have shown that dinuclear platinum(II) acetylides with an A-frame structure, $[Pt_2(\mu\text{-}dppm)_2(\mu\text{-}C{\equiv}C\text{–}R)(C{\equiv}C\text{–}R)_2]^+$ $[R = C_6H_4\text{–}OCH_3\text{-}4$

(**35a**), C_6H_4–CH_2CH_3-4 (**35b**), C_6H_4–OCH_2CH_3-4 (**35c**), C_6H_4–Ph-4 (**35d**), Ph (**35e**), ^{t}Bu (**35f**)], exhibit long-lived intense luminescence both in the solid state and in fluid solutions at room temperature [131,132].

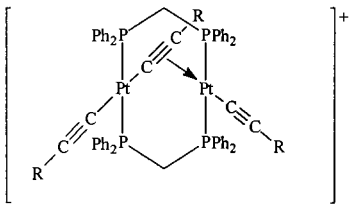

35a: R = C_6H_4-OCH_3-4
35b: R = C_6H_4-CH_2CH_3-4
35c: R = C_6H_4-OCH_2CH_3-4
35d: R = C_6H_4-Ph-4
35e: R = Ph
35f: R = ^{t}Bu

The perspective view of the complex cation of **35e** is shown in Fig. 10. The electronic absorption spectra of complexes **35a**–**f** both in acetonitrile and dichloromethane exhibit similar absorption patterns with a low energy band at ca. 400–450 nm. Such absorption bands are found to be red-shifted with respect to their related monomeric complexes. For example, the 393-nm absorption in **35e** is red-shifted with respect to the 345-nm absorption band in *trans*-[Pt(C≡CPh)$_2$(dppm-*P*)$_2$] while the 391-nm absorption in **35f** is red-shifted with respect to the 329-nm absorption band in *trans*-[Pt(C≡C′Bu)$_2$(dppm-*P*)$_2$]. The absorption band in the monomeric [Pt(dppm)$_2$(C≡CR)$_2$] complex has been assigned as a metal-to-ligand charge-transfer MLCT [d(Pt) → π*(C≡CR)] transition. The occurrence of the absorption band at higher energy in [Pt(C≡C′Bu)$_2$(dppm-*P*)$_2$] than [Pt(C≡CPh)$_2$(dppm-*P*)$_2$] correlates well with the π* orbital energy of the acetylide moieties and lends further support to a MLCT assignment. With reference to previous spectroscopic work on dinuclear d^8–d^8 systems [111–114] and

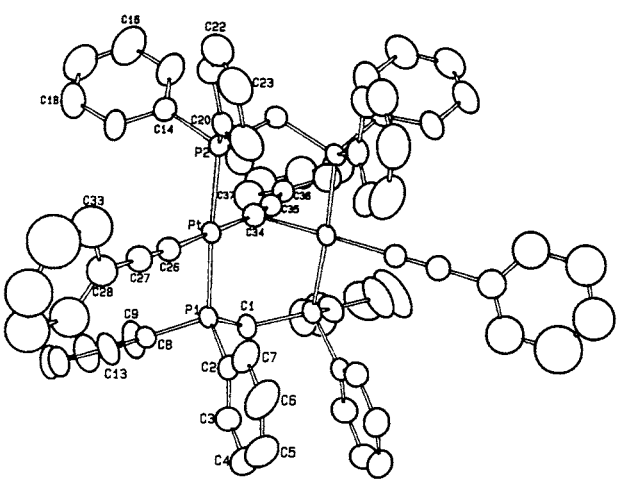

Fig. 10. The perspective view of complex cation of **35e**. Hydrogen atoms have been omitted for clarity.

a related A-frame dinuclear Ir(I) system [133], the absorption band centred at ca. 400–450 nm in the dinuclear species has been assigned as a MMLCT [dσ* → pσ/π*] transition, which is red-shifted with respect to the MLCT [d(Pt) → π*(C≡CR)] transition in the monomeric [Pt(dppm)$_2$(C≡CR)$_2$] complex, where dσ* is the antibonding combination resulting from the interaction of the Pt($5d_{z^2}$)–Pt($5d_{z^2}$) orbitals, while pσ is the bonding combination resulting from the interaction of the Pt($6p_z$)–Pt($6p_z$) orbitals, taking the Pt–Pt bond axis to be the *z*-axis. In view of the low-lying π* orbital energies of the acetylide ligands, it was believed that the LUMO of these dinuclear complexes would have substantial mixing of the π*(acetylide) character with the pσ orbital arising from the $6p_z$–$6p_z$ interaction assuming a C_{2v} symmetry [132]. A similar mixing of the π* character of terminal carbonyls into the LUMO in A-frame complexes has also been reported [133,134]. Spectral assignments similar to this have also been suggested in the related A-frame pyrazolyl-bridged dinuclear iridium(I) complexes [133] and a related [Pt$_2$(dppm)$_2$(CN)$_4$] system [114].

The A-frame dinuclear platinum(II) acetylide complexes exhibit a broad emission band centred at ca. 570–650 nm. The photophysical data are summarized in Table 13. The solid state emission spectra of the complexes **35a**, **35b**, **35d** and **35f** are depicted in Fig. 11. The 77 K solid state emission spectra of **35b**, **35c** and **35d** all show vibronically structured bands with progressional spacing of ca. 2000 cm^{-1}, typical of the ν(C≡C) stretch in the ground state. The 77 K solid-state emission spectra of **35c** and **35d** are shown in Fig. 12. The observation of the vibronic structures is suggestive of the involvement of the acetylide in the transition. A comparison of the 77K solid state emission energy of the complexes, [Pt$_2$(μ-dppm)$_2$(μ-C≡CR)(C≡CR)$_2$]$^+$, shows that the transition energies follow the order: R = C_6H_4–Ph-4 < Ph < C_6H_4–OCH_3-4 ≤ C_6H_4–CH_2CH_3-4 ≤ C_6H_4–OCH_2CH_3-4 < ^{t}Bu, which is in line with the increasing π–π* transition energy of the acetylide ligand, providing further support for the involvement of the π*(C≡CR) orbital in the transition. An assignment of the emissive origin of this class of complex as a pure metal centred ^{3}[(dσ*)(pσ)] state arising from a Pt···Pt interaction similar to those of other dinuclear d^8–d^8 systems has not been favoured, in view of the higher emission energy of **35f** than **35e**, despite the Pt···Pt distance in the former is found to be shorter than that of the latter [3.117(1) Å in **35f** versus 3.236(1) Å in **35e**] [131,135]. A stronger Pt···Pt interaction would have been expected for **35f** based on bond length arguments alone, which should give rise to a lower-lying ^{3}[(dσ*)(pσ)] state.

The emission spectra of the complexes in degassed dichloromethane or acetonitrile show low energy, broad, intense emission bands centred at ca. 620–640

Table 13
Photophysical data for **35a–f**[a]

Complex	Absorption wavelength in CH_3CN λ_{max}/nm (ε/dm^3 mol^{-1} cm^{-1})	Medium (T/K)	Emission wavelength λ_{max}/nm (τ_o/μs)
35a	408 (20,170), 450 (14,690)	Solid (298)	610 (10.0 ± 0.5)
		MeCN (298)	630 (0.10 ± 0.01)
		CH_2Cl_2 (298)	635 (0.20 ± 0.02)
35b	398 (21,790), 440 (12,590)	Solid (298)	590 (11.0 ± 0.5)
		Solid (77)	575, 645 sh
		MeCN (298)	620 (0.15 ± 0.01)
		CH_2Cl_2 (298)	630 (0.14 ± 0.01)
35c	404 (30,160), 460 (16,140)	Solid (298)	595 (9.0 ± 0.5)
		Solid (77)	575, 645 sh
		MeCN (298)	630 (0.15 ± 0.01)
		CH_2Cl_2 (298)	630 (0.20 ± 0.02)
35d	394 (20,360), 436 (14,560)	Solid (298)	635 (5.0 ± 0.5)
		Solid (77)	625
		MeCN (298)	640 (0.9 ± 0.1)
		CH_2Cl_2 (298)	623 (<0.1)
35e	393 (18,170), 450 (7,370)	Solid (298)	618 (2.2 ± 0.2)
		Solid (77)	621
		MeCN (298)	614 (0.11 ± 0.01)
		CH_2Cl_2 (298)	623 (<0.1)
35f	344 (6,480), 375 sh (8,100)	Solid (298)	554 (11 ± 0.5)
		Solid (77)	565
		MeCN (298)	500 (<0.1)

[a] Data from references [131] and [132].

nm. The long luminescence lifetimes in the microsecond range together with the large Stokes shift are suggestive of their phosphorescent nature.

The excitation spectra of the complexes monitored at the emission maxima show excitation maxima well correlated with the absorption maxima of the corresponding complexes. The resemblance of the excitation spectra to the absorption spectra suggests that the emissive state is likely to be derived from a MMLCT origin. The excitation spectrum of **35d** shows two excitation bands at ca. 430 and 480 nm in degassed acetonitrile, tentatively assigned as the $^1[(d\sigma^*)^2] \rightarrow {}^1[(d\sigma^*)^1(p\sigma/\pi^*)^1]$ (singlet–singlet) and $^1[(d\sigma^*)^2] \rightarrow {}^3[(d\sigma^*)^1(p\sigma/\pi^*)^1]$ (singlet–triplet) transitions. The observed energy separation of ca. 2420 cm^{-1} between the singlet–singlet and singlet–triplet transitions is found to be similar to an energy separation of 2198 cm^{-1} for the $^1A_1 \rightarrow {}^1B_1$ and $^1A_1 \rightarrow {}^3B_1$ transitions and 2535 cm^{-1} for the $^1A_1 \rightarrow {}^1A_1$ and $^1A_1 \rightarrow {}^3A_1$ transitions in the related $Ir_2(\mu\text{-}3,5\text{-}Me_2pz)_2(CO)_4$ complex in 2-methylpentane at room temperature (3,5-Me_2pz = 3,5-dimethylpyrazole) [133].

Although the involvement of the π*(C≡CR) orbital in the excited state and the trend in the emission energies upon changing the nature of the acetylide could also be suggestive of an origin derived from an emissive state of intraligand π→π*(C≡CR) character, such an assignment has not been favoured on the grounds that intraligand π→π*(C≡CR) transitions do not usually occur at such low energies and the fact that a red shift in emission energy has been observed upon going from the monomeric $[Pt(dppm)_2(C{\equiv}CR)_2]$ to the corresponding dinuclear A-frame complexes. A MMLCT origin for the emission has been suggested. The assignment has also been supported by resonance Raman spectroscopic studies on **35e** [136]. The resonance Raman spectra of **35e** display almost all of their intensity in fundamental Raman peaks with no appreciable Raman intensity above 2200 cm^{-1} Raman shift. While the resonance Raman spectra of the monomeric $[Pt(dppm)_2(C{\equiv}CPh)_2]$ show only one very strong C≡C stretch peak at ca. 2114 cm^{-1} [137], those of the dinuclear **35e** show three very strong C≡C stretch peaks at 2027, 2062, and 2125 cm^{-1}, corresponding to the three different acetylide

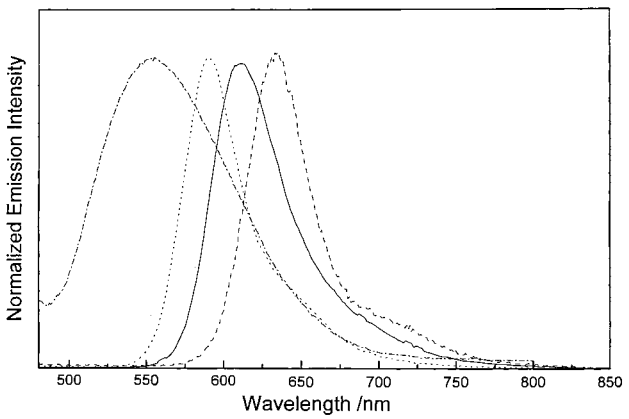

Fig. 11. The solid-state emission spectra of **35a** (—), **35b** (···), **35d** (- - -) and **35f** (- · - · -) at 298 K.

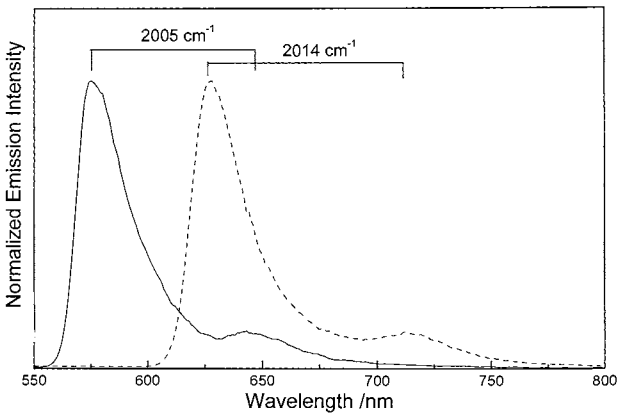

Fig. 12. The solid-state emission spectra of **35c** (—) and **35d** (- - -) at 77 K.

ligand environments. The very similar relative intensities and resonantly enhanced features of the resonance Raman spectra of **35e** as the corresponding monomeric complex MLCT resonance Raman spectra lend additional support for the assignment of the 393-nm absorption band of the dinuclear platinum acetylide complexes to an MMLCT transition and not to an intraligand transition ($\pi \rightarrow \pi^*$ on the C≡CR). Bands at similar energies have also been shown to exhibit large metal-to-ligand charge transfer (MLCT) character in the related A-frame dinuclear iridium(I) complexes [133]. The absolute Raman cross sections for the C≡C peaks with excitation wavelengths within the MLCT absorption band of $[Pt(dppm)_2(C{\equiv}CPh)_2]$ and the MMLCT absorption band of **35e** have been determined [136]. The vibrational reorganization energies for the initially excited MLCT state of $[Pt(dppm)_2(C{\equiv}CPh)_2]$ and MMLCT state of **35e** have been estimated using time-dependent wavepacket calculations [136]. The observation of most of the internal reorganization in the C≡C stretch modes is in line with a MLCT or MMLCT assignment. Emissions from the ^{3}MLCT states of the related complexes $[Pt(PEt_3)_2(C{\equiv}CPh)_2]$ and $[Pt(PEt_3)_2(C \equiv CH)_2]$ exhibit very strong vibrational progressions in the C≡C stretch mode, which are also indicative of a large distortion of the C≡C mode in the ^{3}MLCT states [120].

Bimolecular quenching reactions of the complexes with various pyridinium quenchers have also been studied. An oxidative electron transfer mechanism has been suggested for the quenching reaction. Transient absorption bands at ca. 390 nm characteristic of the pyridinyl radicals have also been observed in laser flash photolysis experiments, confirming the electron transfer nature of these quenching reactions.

A related $[Pt_2(\mu\text{-dppm})_2(\mu\text{-C}{\equiv}C^tBu)(C{\equiv}C^tBu)Cl]^+$ complex has also been shown to exhibit long-lived intense luminescence [131]. An emissive origin similar to that for the $[Pt_2(\mu\text{-dppm})_2(\mu\text{-C}{\equiv}CR)(C{\equiv}CR)_2]^+$ system has been suggested.

The A-frame acetylide complexes $[Pt_2(\mu\text{-dppm})_2(\mu\text{-C}{\equiv}CR)(C{\equiv}CR)_2]^+$ have been found to exhibit fluxional properties [132]. The free energies of activation for the fluxional processes have also been determined.

5. Mixed-metal acetylides

In previous sections, it has been shown that both luminescent copper(I) acetylides and rhenium(I) acetylides are promising building blocks for the construction of rigid-rod oligomeric and polymeric materials. As a further step towords this goal, a series of pentanuclear heterometallic copper(I)-rhenium(I) acetylide complexes $[Cu_3(\mu\text{-P–P})_3\{\mu_3\text{-}\eta^1\text{-C}{\equiv}C{-}C_6H_2\text{-}2,5\text{-}R_2{-}C{\equiv}C\text{-}4{-}Re(N{-}N)(CO)_3\}_2]^+$ [P–P = dppm, N–N = bpy, R = H (**36a**), CH_3 (**36b**); P–P = dppm, N–N = ^{t}Bu$_2$bpy, R = H (**36c**); P–P = $(Ph_2P)_2N{-}CH_2CH_2CH_3$, N–N = bpy, R = H (**36d**), CH_3 (**36e**)] have also been synthesized and their luminescence properties reported by us recently [138,139].

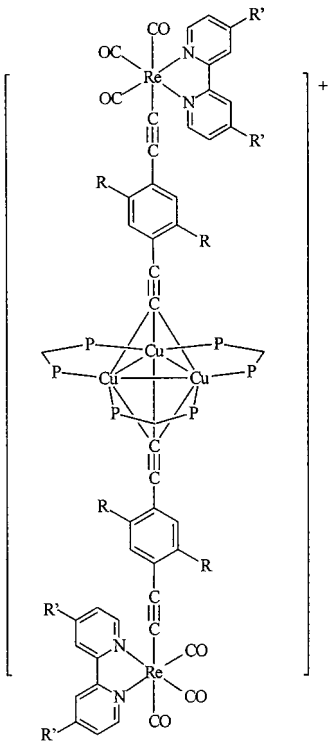

36a: R = R' = H
36b: R = CH_3, R' = H
36c: R = H, R' = ^{t}Bu

P⌒P = dppm

36d: R = R' = H
36e: R = CH_3, R' = H

P⌒P = $(Ph_2P)_2N\text{-}CH_2CH_2CH_3$

The perspective view of the complex cation of **36a** is displayed in Fig. 13. The electronic absorption spectra of the complexes reveal high energy absorption bands at ca. 250–300 nm and vibronically structured bands at ca. 348–378 nm with progressional spacings of ca. 1350–1500 cm^{-1}, typical of aromatic ν(C≡C) stretching frequencies. These transitions are assigned to be ligand-centred in nature. In addition, a lower-energy absorption also occurs at ca. 440 nm, which is likely to be a MLCT [$d\pi(Re) \rightarrow \pi^*(N-N)$] transition. All the mixed-metal acetylide complexes display strong orange luminescence upon photoexcitation. The photophysical data are summarized in Table 14. The low energy emission bands at ca. 600–660 nm have been suggested to arise from a ^{3}MLCT [$(d\pi(Re) \rightarrow \pi^*(N-N)$] excited state. The energy trend of this low energy emission is in line with the $\pi-\pi^*$ transition energies of the diimine ligands. Also, the complexes with more electron-rich $(Ph_2P)_2N-CH_2CH_2CH_3$ phosphine ligands emit at a slightly lower energy compared with the dppm counterparts. This can be rationalized by the fact that the more electron-donating $(Ph_2P)_2N-CH_2CH_2CH_3$ phosphines would render the copper(I) centres more electron-rich, and in turn destablilize the Re(I) dπ orbitals and therefore the ^{3}MLCT [$d\pi(Re) \rightarrow \pi^*(N-N)$] emission occurs at lower energy. The lifetimes of the emission are in the range of submicroseconds which are also common for a rhenium(I) diimine MLCT phosphorescent state. It is interesting to note that upon the addition of rhenium(I) diimine moieties, the character of the lowest-lying excited state of the copper(I) acetylides would change from essentially LMCT [acetylide → copper] to MLCT [rhenium → diimine].

Table 14
Photophysical data for **36a–e**[a]

Complex	Medium (T/K)	Emission wavelength λ_{max}/nm (τ_o/μs)
36a	Solid (298)	616 (<0.1)
	Solid (77)	605
	CH_2Cl_2 (298)	642 (<0.1)
36b	Solid (298)	615 (0.14)
	Solid (77)	608
	CH_2Cl_2 (298)	650 (<0.1)
36c	Solid (298)	613 (0.1)
	Solid (77)	605
	CH_2Cl_2 (298)	615 (<0.1)
36d	Solid (298)	616 (0.12)
	Solid (77)	623[b]
	CH_2Cl_2 (298)	660 (<0.1)
36e	Solid (298)	618 (0.13)
	Solid (77)	615
	CH_2Cl_2 (298)	650 (<0.1)

[a] Data from reference [138].
[b] Excitation wavelength = 510 nm.

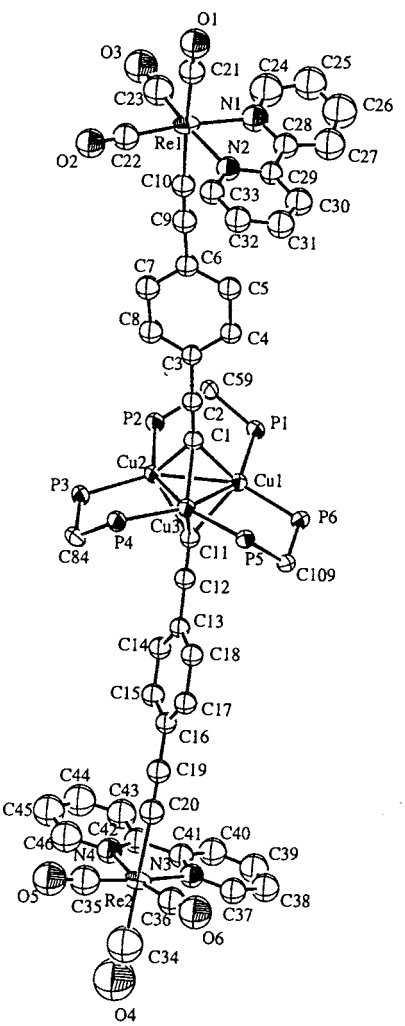

Fig. 13. The perspective view of the complex cation of **36a**. Hydrogen atoms and phenyl rings have been omitted for clarity.

The photophysical properties of a trinuclear heterometallic complex $[Pt(\mu\text{-dppy})_2(\mu\text{-}\eta^1,\eta^2\text{-}C\equiv C\text{-}Ph)_2\{Cu(CH_3CN)_2\}_2]^{2+}$ (**37**) have also been reported [140].

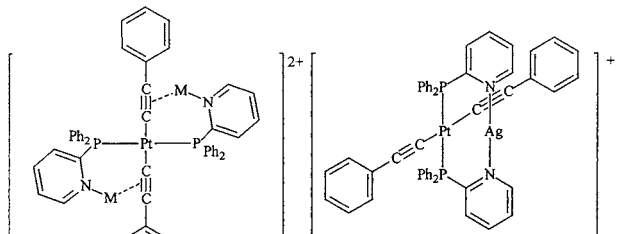

37: M = $Cu(NCCH_3)_2$
38a: M = $Ag(NCCH_3)$
38b

The complex shows absorption shoulders at 265 (ε = 46895 $dm^3\ mol^{-1}\ cm^{-1}$) and 330 nm (ε = 12865 $dm^3\ mol^{-1}\ cm^{-1}$). The lower energy absorption has been assigned to arise from a MLCT [$Pt \rightarrow \pi^*$(acetylide)] transition mixed with some IL $\pi - \pi^*$(acetylide) character. The complex exhibits long-lived luminescence upon photoexcitation. The room-temperature solid-state emission band at 576 nm ($\tau_o = 6.3 \pm 0.6$ μs) has been

proposed to be characteristic of the Pt···Cu systems as both $[Pt(dppy)_2(C{\equiv}C{-}Ph)_2]$ and $[Cu_2(\mu\text{-}dppy)_2(CH_3CN)_2]^+$ emit at a much higher energy. However, in CH_2Cl_2 solution, the complex displays an emission band at 522 nm, which is similar to that of $[Cu_2(\mu\text{-}dppy)_2(CH_3CN)_2]^+$ ($\lambda_{max} = 533$ nm). The origin of this emission band has been assigned to be ^{3}MLCT [Cu → π*(dppy)] in nature. The absence of Pt···Cu perturbation has been ascribed to the non-rigidity of the trinuclear heterometallic complex in fluid solution.

The photophysical properties of related complexes $[Pt(\mu\text{-}dppy)_2(\mu\text{-}\eta^1,\eta^2\text{-}C{\equiv}C{-}Ph)_2\{Ag(CH_3CN)_2\}_2]^{2+}$ (**38a**) and $[Pt(\mu\text{-}dppy)_2(C{\equiv}C{-}Ph)_2Ag]^+$ (**38b**) have been reported [140]. The complexes show a high energy absorption shoulder at ca. 260 nm and a lower absorption band at ca. 350 nm. The latter has been assigned to arise from the MLCT [Pt → π*(acetylide)] transition, and perhaps mixed with some IL π–π*(acetylide) character. Upon photoexcitation, the complexes display long-lived solid-state emission at 501 nm ($\tau_o = 5.7 \pm 0.3$ μs) and 555 nm ($\tau_o = 1.0 \pm 0.1$ μs), respectively at 298 K. The origin of the former has been assigned to an IL π–π*(dppy)/MLCT [Ag → π*(dppy)] triplet state. In CH_2Cl_2 solution, complexes **38a** and **38b** also reveal low energy emission bands at 588 nm and 640 nm, respectively. These emission bands have been proposed to be characteristic of the Pt···Ag interaction.

The photophysical properties and the electronic structure of the heterometallic complex $[AgPt(\mu\text{-}dppm)_2(C{\equiv}C{-}Ph)_2]^+$ (**39a**) have also been described [122].

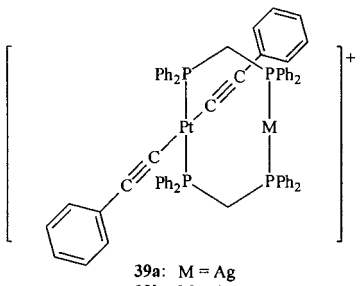

39a: M = Ag
39b: M = Au

The complex exhibits strong absorption bands at 318 nm ($\varepsilon = 1.71 \times 10^4$ dm^3 mol^{-1} cm^{-1}) and 368 nm ($\varepsilon = 1.63 \times 10^4$ dm^3 mol^{-1} cm^{-1}) which are assigned to spin-allowed [1π → 1π*] and [d_{σ^*}(Ag–Pt) → 1π*] transitions, respectively, where 1π denotes the mixed-orbital of acetylide (π) and Pt($5d_{yz}$), and 1π* denotes the mixed-orbital of acetylide (π*) and Pt($6p_z$) (the Ag–Pt vector was taken to be the z-axis and the P–Pt–P vector to be the x-axis). The d_{σ^*} orbital arises from the anti-bonding interaction between Ag($4d_{z^2}$) and Pt($5d_{z^2}$) orbitals. Upon photoexcitation, the emission of the complex in the solid state occurs at 495 nm ($\tau_o = 0.2$ μs) at 298 K. At 77 K, the complex in alcohol glass emits at 449 nm with a vibronically structured emission band of progressional spacings of ca. 2000–2110 cm^{-1}, typical of the stretching frequencies of the coordinated phenylacetylide ligand, indicative of the participation of the ligand in the excited state characteristic of the complex.

The spectroscopic and luminescence properties of a related gold(I)–platinum(II) complex $[AuPt(\mu\text{-}dppm)_2(C{\equiv}C{-}Ph)_2]^+$ (**39b**) have also been reported [122]. X-ray crystallographic studies reveal a gold–platinum separation of 2.910(1) Å. The electronic absorption spectrum of the complex in CH_3CN display intense absorption bands at 329 nm ($\varepsilon = 1.64 \times 10^4$ dm^3 mol^{-1} cm^{-1}) and 387 nm ($\varepsilon = 1.11 \times 10^4$ dm^3 mol^{-1} cm^{-1}), which are assigned to spin-allowed [1π → 1π*] and [d_{σ^*}(Au–Pt) → 1π*] transitions, respectively, where 1π denotes the mixed-orbital of acetylide (π) and Pt($5d_{yz}$), and 1π* denotes the mixed-orbital of acetylide (π*) and Pt($6p_z$) (the Au–Pt vector was taken to be the z-axis and the P–Pt–P vector to be the x-axis). The d_{σ^*} orbital arises from the anti-bonding interaction between $5d_{z^2}$ orbitals of Au and Pt. The occurrence of the [d_{σ^*}(Au–Pt) → 1π*] transition at a lower energy than the [d_{σ^*}(Ag–Pt) → 1π*] transition of the silver(I)–platinum(II) analogue **39a** is in line with a stronger Au–Pt interaction than the Ag–Pt interaction, as suggested by X-ray crystallographic data.

The solid-state emission spectrum of the Au–Pt complex **39b** shows a narrow peak at 462 nm and a shoulder at 510 nm, both show monoexponential decay with a lifetime of 0.35 μs. At 77 K EtOH/MeOH (4:1 v/v) glass, the complex emits at 454 nm with a shoulder at 502 nm. The emission appears to be vibronically structured, with a progressional spacing of 2106 cm^{-1}, typical of ground-state ν(C≡C) stretching. The excitation spectrum obtained by monitoring at 450 nm shows two bands at ca. 320–350 and 390 nm which are suggested to correspond to the ^{1}[1π → 1π*] and ^{1}[d_{σ^*} → 1π*] transitions, respectively.

6. Conclusion

This review article summarizes the recent work on the photophysics and photochemistry of polynuclear transition metal acetylides by us and other research groups. In the search for novel luminescent materials, it is found that while there are a lot of metal acetylide complexes in the literature, the photophysical and photochemical properties of this class of organometallics are comparatively unexplored. It is expected that with acetylides as ligands, which show a variety of different bonding modes, isolation of polynuclear metal acetylide complexes with novel molecular structures is promising. Most of these metal acetylides are also found to exhibit rich and remarkable photoluminescence properties that are unique to this class of compounds.

Copper(I), silver(I) and gold(I) acetylides are well known to exist in the form of clusters or aggregates.

The acetylide complexes of these metal centres included in this review are strongly luminescent with a long-lived excited state. The most remarkable feature of this class of luminescent materials is the identification of a ligand-to-metal charge-transfer (LMCT) excited state mixed with a metal-centred (MC) ds/dp state; the relative contribution of which depends on the nature of the acetylide ligand and the extent of the metal–metal interaction. An emission originating from a LMCT excited state is extremely rare compared to that of the MLCT counterparts. In the presence of electron-rich acetylide ligands and empty $(n+1)$s and $(n+1)$p orbitals of the nd^{10} metal centres, these polynuclear d^{10} metal acetylides have been demonstrated to exhibit long-lived LMCT/MC ds/dp excited states, shown by systematic alteration of the ligands and metal centres. The rich photoredox properties of these luminescent complexes have also been revealed by their photoinduced electron-transfer reactions with different electron acceptors.

The photochemistry of rhenium(I) diimine and platinum(II) phosphine complexes has also attracted a lot of interest. However, corresponding studies on those systems containing acetylide ligands have gained little attention. One advantage of incorporating acetylides into these complexes lies in the strong electron-donating properties of acetylides, which would raise the energies of the metal-centred d–d states such that any nonradiative deactivation pathways due to the presence of low-lying ligand-field d–d states could be suppressed. Incorporation of different diimine and/or acetylide ligands to the rhenium(I) and platinum(II) centres also enables the fine tuning of the photoluminescence energy, which is exceptionally important in the realization of supramolecular electron- and energy-transfer systems.

In conclusion, these luminescent polynuclear metal acetylide complexes represent an extension of inorganic photochemistry from Werner-type coordination compounds to organometallic systems. Meanwhile, they also open up a completely new dimension of organometallic photochemistry. It is anticipated that exploration in this area will lead to an important aspect of photochemistry. Moreover, a thorough understanding on the fundamental aspects of the photophysical and photochemical properties of these luminescent organometallic complexes would lead to the production of novel luminescent materials and would provide model systems for the development of light-emitting diodes, new materials with non-linear optical properties and liquid crystalline properties.

References

[1] G.H. Posner, An Introduction to Synthesis using Organocopper Reagents, Krieger, Malabar, FL, 1988.
[2] B.H. Lipshutz (Ed.), Recent developments in Organocopper Chemistry, Tetrahedron 45 (1989) 349–534.
[3] P.P. Power, Prog. Inorg. Chem. 39 (1991) 75.
[4] N. Krause, A. Gerold, Angew. Chem. Int. Ed. Engl. 36 (1997) 187.
[5] B.J. Hathaway, in: G. Wilkinson, R.D. Gillard, J.A. McCleverty (Eds.), Comprehensive Coordination Chemistry, vol. 5, Pergamon, Oxford, 1987, pp. 533–774.
[6] G. van Koten, S.L. James, J.T.B.H. Jastrzebski, in: E.W. Abel, F.G.A. Stone, G. Wilkinson (Eds.), Comprehensive Organometallic Chemistry II, vol. 3, Pergamon, Oxford, 1995, pp. 57–133.
[7] M.P. Gamasa, J. Gimeno, E. Lastra, A. Aguirre, S. García-Granda, J. Organomet. Chem. 378 (1989) C11.
[8] J. Diéz, M.P. Gamasa, J. Gimeno, A. Aguirre, S. García-Granda, Organometallics 10 (1991) 380.
[9] V.W.W. Yam, J. Photochem. Photobiol. A Chem. 106 (1997) 75.
[10] V.W.W. Yam, K.K.W. Lo, W.K.M. Fung, C.R. Wang, Coord. Chem. Rev. 171 (1998) 17.
[11] V.W.W. Yam, W.K. Lee, T.F. Lai, Organometallics 12 (1993) 2383.
[12] V.W.W. Yam, W.K. Lee, P.K.Y. Yeung, D. Phillips, J. Phys. Chem. 98 (1994) 7545.
[13] V.W.W. Yam, W.K. Lee, K.K. Cheung, B. Crystall, D. Phillips, J. Chem. Soc. Dalton Trans. (1996) 3283.
[14] V.W.W. Yam, W.K. Lee, K.K. Cheung, J. Chem. Soc. Dalton Trans. (1996) 2335.
[15] V.W.W. Yam, S.W.K. Choi, C.L. Chan, K.K. Cheung, Chem. Commun. (1996) 2067.
[16] V.W.W. Yam, W.K.M. Fung, K.K. Cheung, Angew. Chem. Int. Ed. Engl. 35 (1996) 1100.
[17] V.W.W. Yam, W.K. Lee, K.K. Cheung, H.K. Lee, W.P. Leung, J. Chem. Soc. Dalton Trans. (1996) 2889.
[18] V.W.W. Yam, W.K.M. Fung, M.T. Wong, Organometallics 16 (1997) 1772.
[19] V.W.W. Yam, W.K.M. Fung, K.K. Cheung, Chem. Commun. (1997) 963.
[20] V.W.W. Yam, W.K.M. Fung, K.K. Cheung, Organometallics 17 (1998) 3293.
[21] V.W.W. Yam, W.K.M. Fung, K.K. Cheung, J. Cluster Sci. (1999) in press.
[22] J. Hermolin, M. Levin, E.M. Kosower, J. Am. Chem. Soc. 103 (1981) 4808.
[23] J. Hermolin, M. Levin, Y. Ikegami, M. Sawayanagi, E.M. Kosower, J. Am. Chem. Soc. 103 (1981) 4795.
[24] A.B.P. Lever, Inorganic Electronic Spectroscopy, 2nd ed., Elsevier, Amsterdam, 1984.
[25] M.B. Robin, P. Day, Adv. Inorg. Chem. Radiochem. 10 (1967) 247.
[26] R.R. Gagné, C.A. Koval, T.J. Smith, J. Am. Chem. Soc. 99 (1977) 8367.
[27] R.R. Gagné, C.A. Koval, T.J. Smith, M.C. Cimolino, J. Am. Chem. Soc. 101 (1979) 4571.
[28] C. Harding, V. McKee, J. Nelson, J. Am. Chem. Soc. 113 (1991) 9684.
[29] B. Scott, R. Willett, L. Porter, J. Williams, Inorg. Chem. 31 (1992) 2483.
[30] M.E. Barr, P.H. Smith, W.E. Antholine, B. Spencer, J. Chem. Soc. Chem. Commun. (1993) 1649.
[31] I.S. Delsahüt, B.L. Loeb, J. Coord. Chem. 33 (1994) 33.
[32] V.W.W. Yam, K.K.W. Lo, C.R. Wang, K.K. Cheung, J. Phys. Chem. A 101 (1997) 4666.
[33] V.W.W. Yam, K.K.W. Lo, Comments Inorg. Chem. 19 (1997) 209.
[34] L. Naldini, F. Demartin, M. Manassero, M. Sansoni, G. Rassu, M.A. Zoroddu, J. Organomet. Chem. 279 (1985) C42.

[35] R.J. Lancashire, in: G. Wilkinson, R.D. Gillard, J.A. McCleverty (Eds.), Comprehensive Coordination Chemistry, vol. 5, Pergamon, 1987, Oxford, 1987, pp. 775–859.
[36] V.W.W. Yam, W.K.M. Fung, K.K. Cheung, Organometallics 16 (1997) 2032.
[37] C.F. Wang, S.M. Peng, C.K. Chan, C.M. Che, Polyhedron 15 (1996) 1853.
[38] A. Bondi, J. Phys. Chem. 68 (1964) 441.
[39] C.E. Moore, Natl. Stand. Ref. Data Series (U.S. Natl. Bur. Stand.) 35 (1971) p. 51, 116.
[40] R.J. Puddephatt, in: G. Wilkinson, R.D. Gillard, J.A. McCleverty (Eds.), Comprehensive Coordination Chemistry, vol. 5, Pergamon, 1987, Oxford, 1987, pp. 861–923.
[41] A. Grohmann, H. Schmidbaur, in: E.W. Abel, F.G.A. Stone, G. Wilkinson (Eds.), Comprehensive Organometallic Chemistry II, vol. 3, Pergamon, 1995, Oxford, 1995, pp. 1–56.
[42] R.J. Puddephatt, Chem. Commun. (1998) 1055.
[43] C. King, J.C. Wang, M.N.I. Khan, J.P. Fackler Jr., Inorg. Chem. 28 (1989) 2145.
[44] C.M. Che, H.L. Kwong, C.K. Poon, V.W.W. Yam, J. Chem. Soc. Dalton Trans. (1990) 3215.
[45] V.W.W. Yam, T.F. Lai, C.M. Che, J. Chem. Soc. Dalton Trans. (1990) 3747.
[46] V.W.W. Yam, W. K. Lee, J. Chem. Soc. Dalton Trans. (1993) 2097.
[47] T.M. McCleskey, H.B. Gray, Inorg. Chem. 31 (1992) 1733.
[48] B. Weissbart, D.V. Toronto, A.L. Balch, D.S. Tinti, Inorg. Chem. 35 (1996) 2490.
[49] V.W.W. Yam, S.W.K. Choi, J. Chem. Soc. Dalton Trans. (1994) 2057.
[50] J.C. Vickery, M.M. Olmstead, E.Y. Fung, A.L. Balch, Angew. Chem. Int. Ed. Engl. 36 (1997) 1179.
[51] D. Li, X. Hong, C.M. Che, W.C. Lo, S.M. Peng, J. Chem. Soc. Dalton Trans. (1993) 2929.
[52] C.M. Che, H.K. Yip, W.C. Lo, S.M. Peng, Polyhedron 13 (1994) 887.
[53] S.J. Shieh, X. Hong, S.M. Peng, C.M. Che, J. Chem. Soc. Dalton Trans. (1994) 3067.
[54] V.W.W. Yam, S.W.K. Choi, J. Chem. Soc. Dalton Trans. (1996) 4227.
[55] V.W.W. Yam, S.W.K. Choi, K.K. Cheung, Organometallics 15 (1996) 1734.
[56] V.W.W. Yam, S.W.K. Choi, K.K. Cheung, J. Chem. Soc. Dalton Trans. (1996) 3411.
[57] X. Hong, K.K. Cheung, C.X. Guo, C.M. Che, J. Chem. Soc. Dalton Trans. (1994) 1867.
[58] T.E. Müller, S.W.K. Choi, D.M.P. Mingos, D. Murphy, D.J. Williams, V.W.W. Yam, J. Organomet. Chem. 484 (1994) 209.
[59] H. Xiao, K.K. Cheung, C.M. Che, J. Chem. Soc. Dalton Trans. (1996) 3699.
[60] B.C. Tzeng, W.C. Lo, C.M. Che, S.M. Peng, Chem. Commun. (1996) 181.
[61] M.J. Irwin, J.J. Vittal, R.J. Puddephatt, Organometallics 16 (1997) 3541.
[62] M. Appel, J. Heidrich, W. Beck, Chem. Ber. 120 (1987) 1087.
[63] J. Heidrich, M. Steimann, M. Appel, W. Beck, Organometallics 9 (1990) 1296.
[64] S. Mihan, T. Weidmann, V. Weinrich, D. Fenske, W. Beck, J. Organomet. Chem. 541 (1997) 423.
[65] T. Weidmann, V. Weinrich, B. Wagner, C. Robl, W. Beck, Chem. Ber. 124 (1991) 1363.
[66] A. Wong, J.A. Gladysz, J. Am. Chem. Soc. 104 (1982) 4948.
[67] J.J. Kowalczyk, A.M. Arif, J.A. Gladysz, Organometallics 10 (1991) 1079.
[68] D.R. Senn, A. Wong, A.T. Patton, M. Marsi, C.E. Strouse, J.A. Gladysz, J. Am. Chem. Soc. 110 (1988) 6096.
[69] J.A. Ramsden, F. Agbossou, D.R. Senn and J.A. Gladysz, J. Chem. Soc. Chem. Commun. (1991) 1360.
[70] Y. Zhou, J.W. Seyler, W. Weng, A.M. Arif, J.A. Gladysz, J. Am. Chem. Soc. 115 (1993) 8509.
[71] J.W. Seyler, W. Weng, Y. Zhou, J.A. Gladysz, Organometallics 12 (1993) 3802.
[72] M. Brady, W. Weng, J.A. Gladysz, J. Chem. Soc. Chem. Commun. (1994) 2655.
[73] T. Bartik, B. Bartik, M. Brady, R. Dembinski, J.A. Gladysz, Angew. Chem. Int. Ed. Engl. 35 (1996) 414.
[74] M. Brady, W. Weng, Y. Zhou, J.W. Seyler, A.J. Amoroso, A.M. Arif, M. Böhme, G. Frenking, J.A. Gladysz, J. Am. Chem. Soc. 119 (1997) 775.
[75] W. Weng, T. Bartik, J.A. Gladysz, Angew. Chem. Int. Ed. Engl. 33 (1994) 2199.
[76] W. Weng, T. Bartik, M. Brady, B. Bartik, J.A. Ramsden, A.M. Arif, J.A. Gladysz, J. Am. Chem. Soc. 117 (1995) 11922.
[77] A.A. Koridze, A.A. Kizas, N.E. Kolobova V.N. Vinogrdova N.A. Ustynyuk, P.V. Petrovskii, A.I. Yanovsky, Y.T. Struchkov, J. Chem. Soc. Chem. Commun. (1984) 1158.
[78] A.D. Shaposhnikova, R.A. Stadnichenko, G.L. Kamalov, A.A. Pasynskii, I.L. Eremenko, S.E. Nefedov, Y.T. Struchkov, A.I. Yanovsky, J. Organomet. Chem. 453 (1993) 279.
[79] A.A. Koridze, V.I. Zdanovich, O.A. Kizas, A.I. Yanovsky, Y.T. Struchkov, J. Organomet. Chem. 464 (1994) 197.
[80] K.W. Lee, W.T. Pennington, A.W. Cordes, T.L. Brown, J. Am. Chem. Soc. 107 (1985) 631.
[81] M.S. Wrighton, D.L. Morse, J. Am. Chem. Soc. 96 (1974) 998.
[82] V. Balzani, F. Scandola, A Supramolecular Photochemistry, Ellis-Horwood, Chichester, 1991.
[83] K. Kalyanasundaram, Photochemistry of Polypyridine and Porphyrin Complexes, Academic Press, London, 1992.
[84] O. Horváth, K.L. Stevenson, Charge Transfer Photochemistry of Coordination Compounds, VCH, New York, 1993.
[85] S.M. Fredericks, J.C. Luong, M.S. Wrighton, J. Am. Chem. Soc. 101 (1979) 7415.
[86] J.V. Caspar, B.P. Sullivan, T.J. Meyer, Inorg. Chem. 23 (1984) 2104.
[87] B.P. Sullivan, C.M. Bolinger, D. Conrad, W.J. Vining, T.J. Meyer, J. Chem. Soc. Chem. Commun. (1985) 1414.
[88] G.T. Tapolsky, R. Duesing, T.J. Meyer, Inorg. Chem. 97 (1987) 2285.
[89] A.J. Lees, Chem. Rev. 29 (1990) 711.
[90] S.V. Wallendael, R.J. Shaver, D.P. Rillema, B.J. Yoblinski, M. Stathis, T.F. Guarr, Inorg. Chem. 29 (1990) 1761.
[91] D.J. Stufkens, Comments Inorg. Chem. 13 (1992) 359.
[92] V.W.W. Yam, V.C.Y. Lau, K.K. Cheung, J. Chem. Soc. Chem. Commun. (1995) 259.
[93] V.W.W. Yam, V.C.Y. Lau, L.X. Wu, J. Chem. Soc. Dalton Trans. (1998) 1461.
[94] V.W.W. Yam, K.K.W. Lo, K.K. Cheung, R.Y.C. Kong, J. Chem. Soc. Dalton Trans. (1997) 2067.
[95] H.D. Stoeffler, N.B. Thornton, S.L. Temkin, K.S. Schanze, J. Am. Chem. Soc. 117 (1995) 7119.
[96] N.B. Thornton, K.S. Schanze, New J. Chem. 20 (1996) 791.
[97] V.W.W. Yam, K.M.C. Wong, V.W.M. Lee, K.K.W. Lo, K.K. Cheung, Organometallics 14 (1995) 4034.
[98] Y. Shen, B.P. Sullivan, Inorg. Chem. 34 (1995) 6235.
[99] V.W.W. Yam, A.S.F. Kai, Chem. Commun. (1998) 109.
[100] V.W.W. Yam, V.C.Y. Lau, K.K. Cheung, Organometallics 14 (1995) 2749.
[101] V.W.W. Yam, V.C.Y. Lau, K.K. Cheung, Organometallics 15 (1996) 1740.
[102] D.L. Lichtenberger, S.K. Renshaw, R.M. Bullock, J. Am. Chem. Soc. 115 (1993) 3276.
[103] D.L. Lichtenberger, S.K. Renshaw, A. Wong, C.D. Tagge, Organometallics 12 (1993) 3522.

[104] J. Manna, S.J. Geib, M.D. Hopkins, Angew. Chem. Int. Ed. Engl. 32 (1993) 858.
[105] J.C. Luong, H. Faltynek, M.S. Wrighton, J. Am. Chem. Soc. 101 (1979) 1597.
[106] L.A. Lucia, R.D. Burton, K.S. Schanze, Inorg. Chim. Acta 208 (1993) 103.
[107] T.J. Meyer, Acc. Chem. Res. 22 (1989) 163.
[108] V.W.W. Yam, K.M.C. Wong, unpublished results.
[109] V.W.W. Yam, S.H.F. Chong, K.K. Cheung, Chem. Commun. (1998) 2121.
[110] J. Manna, K.D. John, M.D. Hopkins, Adv. Organomet. Chem. 38 (1995) 79.
[111] C.M. Che, L.G. Butler, H.B. Gray, J. Am. Chem. Soc. 103 (1981) 7796.
[112] D.M. Roundhill, H.B. Gray, C.M. Che, Acc. Chem. Res. 22 (1989) 55.
[113] A.P. Zipp, Coord. Chem. Rev. 84 (1988) 47.
[114] C. M. Che, V.W.W. Yam, W.T. Wong, T.F. Lai, Inorg. Chem. 28 (1989) 758.
[115] E. Baralt, E.A. Boudreaux, J.N. Demas, P.G. Lenhert, C.M. Lukehart, A.T. McPhail, D.R. McPhail, J.B. Myers, L. Sacksteder, W.R. True, Organometallics 8 (1989) 2417.
[116] J.V. Caspar, J. Am. Chem. Soc. 107 (1985) 6718.
[117] P.D. Harvey, H.B. Gray, J. Am. Chem. Soc. 110 (1988) 2145.
[118] W.A. Fordyce, G.A. Crosby, Inorg. Chem. 21 (1982) 1455.
[119] L. Sacksteder, E. Baralt, B.A. DeGraff, C.M. Lukehart, J.N. Demas, Inorg. Chem. 30 (1991) 3955.
[120] L. Sacksteder, E. Baralt, B.A. DeGraff, C.M. Lukehart, J.N. Demas, Inorg. Chem. 30 (1991) 2468.
[121] H. Masai, K. Sonogashira, N. Hagihara, Bull. Chem. Soc. Jpn. 44 (1971) 2226.
[122] H.K. Yip, H.M. Lin, Y. Wang, C.M. Che, J. Chem. Soc. Dalton Trans. (1993) 2939.
[123] C.W. Chan, L.K. Cheng, C.M. Che, Coord. Chem. Rev. 132 (1994) 87.
[124] S.L. James, M. Younus, P.R. Raithby, J. Lewis, J. Organomet. Chem. 543 (1997) 233.
[125] J. Lewis, M.S. Khan, A.K. Kakkar, B.F.G. Johnson, T.B. Marder, H.B. Fyfe, F. Wittmann, R.H. Friend, A.E. Dray, J. Organomet. Chem. 425 (1992) 165.
[126] N. Chawdhury, A. Köhler, R.H. Friend, M. Younus, N.J. Long, P.R. Raithby, J. Lewis, Macromolecules 31 (1998) 722.
[127] S. Kotani, K. Shiina, K. Sonogashira, Appl. Organomet. Chem. 5 (1991) 417.
[128] K. Sonogashira, S. Kataoka, S. Takahashi, N. Hagihara, J. Organomet. Chem. 160 (1978) 319.
[129] S. Takahashi, H. Morimoto, E. Murata, S. Kataoka, K. Sonogashira, N. Hagihara, J. Polym. Sci.: Polym. Chem. Ed. 20 (1982) 565.
[130] T. Tahara, K. Seto, S. Takahashi, Polym. J. 19 (1987) 301.
[131] V.W.W. Yam, L.P. Chan, T.F. Lai, Organometallics 12 (1993) 2197.
[132] V.W.W. Yam, P.K.Y. Yeung, L.P. Chan, W.M. Kwok, D.L. Phillips, K.L. Yu, R.W.K. Wong, H. Yan, Q.J. Meng, Organometallics 17 (1998) 2590.
[133] J.L. Marshall, M.D. Hopkins, V.M. Miskowski, H.B. Gray, Inorg. Chem. 31 (1992) 5034.
[134] D.M. Hoffman, R. Hoffmann, Inorg. Chem. 20 (1981) 3543.
[135] N.W. Alcock, T.J. Kemp, P.G. Pringle, P. Bergamini, O. Traverso, J. Chem. Soc. Dalton Trans. (1987) 1659.
[136] W.M. Kwok, D.L. Phillips, P.K.Y. Yeung, V.W.W. Yam, J. Phys. Chem. A 101 (1997) 9286.
[137] W.M. Kwok, D.L. Phillips, P.K.Y. Yeung, V.W.W. Yam, Chem. Phys. Lett. 262 (1996) 699.
[138] V.W.W. Yam, W.K.M. Fung, K.M.C. Wong, V.C.Y. Lau, K.K. Cheung, Chem. Commun. (1998) 777.
[139] V.W.W. Yam, W.K.M. Fung, K.M.C. Wong, V.C.Y. Lau, K.K. Cheung, unpublished results.
[140] V.W.W. Yam, L.P. Chan, T.F. Lai, J. Chem. Soc. Dalton Trans. (1993) 2075.